ADSORPTION OF AROMATIC SULFUR COMPOUNDS ON METAL-ORGANIC FRAMEWORKS (MOFs)

by

MUSLUM DEMIR

A Thesis submitted to the

Graduate School-Camden

Rutgers, The State University of New Jersey

in partial fulfillment of the requirements

for the degree of

Master of Science

Graduate Program in Chemistry

written under the direction of

Dr. ALEXANDER SAMOKHVALOV

and approved by

_____

Dr. Alexander Samokhvalov

_____

Dr. Alex J. Roche

_____

Dr. George Kumi

Camden, New Jersey

May 2013

i

Abstract of the Thesis

Adsorption of Aromatic Sulfur Compounds on Metal-Organic Frameworks (MOFs)

By MUSLUM DEMIR

Dissertation Director:

Professor ALEXANDER SAMOKHVALOV

Large-ring aromatic sulfur compounds, e.g., benzothiophene (BT), dibenzothiophene (DBT), present in petroleum and liquid fuels are harmful to human health and the environment. These compounds cause acid rain due to SO_2 formation upon combustion of liquid fossil fuels. We studied the use of Metal Organic Frameworks (MOFs), e.g., Cu-MOF Basolite C300, to remove aromatic sulfur compounds from model liquid fossil fuels in a selective way and in a non-destructive fashion. The kinetics of the adsorption of aromatic sulfur compounds on Copper-MOF (Cu-MOF) was investigated under ambient conditions. The adsorption capacity of Cu-MOF with respect to large-ring aromatic sulfur compounds was examined under thermodynamic equilibrium at different temperatures. The chemical analysis of the liquid phase was performed by UV/VIS spectroscopy (quantitative determination) and high performance liquid chromatography HPLC (qualitative chemical analysis). Also, quantum chemical simulations of the structure of the aromatic sulfur compound DBT and its molecular spectra were conducted. In addition, evidence of a molecular interaction between MOFs and aromatic sulfur compounds was shown by fluorescence spectroscopy.

Acknowledgements and Dedication

I would like to express my gratitude to Dr. Alexander Samokhvalov, who was my M.S. thesis advisor, for his ideas and guidance on this entire dissertation. I would also like to thank my M.S. Committee members: Dr. Alex J. Roche and Dr. George Kumi for their help with editing my dissertation. I am grateful to the Turkish government for funding my graduate work. In particular, I would like to thank the Turkish Educational Attaché at New York for their constant support and mentorship. I thank the Department of Chemistry Faculty, Staff, and fellow Graduate Students whom I had the pleasure to work with during my Graduate studies at Rutgers University.

This Research and thesis dedicated to;

My father Temo DEMIR, without your sacrifices, this would not have been possible. Thank you for constantly supporting me throughout this process.

Table of Contents

List of Figures

List of Tables

Chapter 1: Introduction

1.1 Fossils, Petroleum and Clean Fuels

The world takes many rigorous steps to standardize sulfur emissions. There are many reasons for lowering sulfur levels in liquid fuels. Firstly, the combustion of sulfur compounds present in liquid fuels produces harmful gases, which can react with water to form sulfurous and sulfuric acids. These acid rains are harmful to our health systems, environment, and economy. Acid rain is corrosive and causes damage to plants, roofs of homes, cars, trucks, metal structures, and cement. Moreover, acid rain is an irritant to several organs, such as the heart, and it causes many illnesses and diseases, such as asthma and bronchitis. Aromatic sulfur compounds can contaminate water and soil sources. Furthermore, these sulfur compounds contribute to chemical substances which cause smog.

The emission control system of trucks and cars requires lower than 40 parts per million weight (ppmw) amounts of sulfur compounds in liquid fuels [1]. Before any removal of sulfur compounds from crude oil, the total sulfur levels can be in the range of 100 to 33,000 ppmw. Thus, the EPA (Environmental Protection Agency) has certain limitations on the sulfur levels present in petroleum. In the USA, the law states that the levels of total sulfur in transportation fuels must not be higher than 15 ppmw for diesel fuel and not higher than 30 ppmw for gasoline. For some applications, e.g., fuel cells, 'zero sulfur' fuels (total sulfur content < 1 ppmw) that require an ultradeep desulfurization process are needed [2]. According to the EURO IX standard, sulfur content is required to be less than 50 ppmw in diesel fuel for most highway vehicles.

However, ULSD (ultra low sulfur diesel) is now required to contain a maximum of 10 ppmw total sulfur, which is similar to the new Euro V standard of 2009 [3].

Several criteria must be considered in the ultra-desulfurization of liquid fuels. The first one is capital cost, in which lower unit operation, minimum equipment, and cheaper materials are taken into account in order to keep prices inexpensive. The second one is operation cost, in which the use of hydrogen and the generation of waste should be minimized. The product volume capacity must be as high as 99 percent and the process cycle life should be sufficiently long enough. Also, the operation system should be simple and use the least amount of catalysts [4].

Table 1: Sulfur levels for gasoline and diesel [5]

Country/Region	Fuel	Year	Sulfur limit (ppmw)
USA	Gasoline	2006	30
USA	Diesel	2006	15
European Union	Gasoline, Diesel	2009	10
China	Gasoline	2005	<350
China	Diesel	2005	<150

1.2 Aromatic Sulfur Compounds

Heteroaromatic sulfur-containing organic compounds such as alkyl-substituted thiophene, benzothiophenes (BT), and dibenzothiophenes (DBT) are the abundant components of fossils and fossil fuels, such as petroleum [6], oil shale [7], tar sands [8], bitumen [9]. The content of sulfur in crude petroleum is between about 100 [10] and 80,000 ppmw [11]. Many aromatic sulfur compounds, such as thiophene, BT, and DBT, can be found in products of petroleum refining and upgrading, such as napthas [12] and gas oils [13]. Aromatic sulfur compounds are also present in commercial products of processing of fossils such as gasoline [14], diesel, and jet fuels. With significant recent developments, the molecular structure and the concentration of representative aromatic sulfur compounds have been determined in petroleum [15], refinery naphthas [11], oils [13], and commercial liquid fuels [16].

Heteroaromatic polymers present in brown coals have major structural units that are similar to those of aromatic sulfur compounds. Thus, coal liquefaction produces liquid fuels that contain a high concentration of aromatic sulfur compounds. When fossil fuels containing sulfur compounds are burned, sulfur is released as sulfur dioxide SO_2 [17] and as direct particulate matter (DPM) containing sulfur [18]. Once in the air, sulfur compounds pose a serious health hazard and cause malfunctioning of all major pollution control technologies, such as automobile catalytic converters [18]. Similarly, incomplete burning of transportation fuels releases toxic aromatic sulfur compounds into the air [19]. The liquid waste of refineries also contains a significant concentration of aromatic sulfur compounds. The major source of contamination by aromatic sulfur compounds is crude petroleum spills [20], for example the recent oil leak in the Gulf of Mexico [21]. Some of

the most harmful and toxic compounds found in marine environments include methyl-substituted aromatic sulfur compounds [22]. Aromatic sulfur compounds are also present outside of fossil fuels in molecules of certain organic semiconductors, pesticides, drugs, components of the soil, and human body (pheomelanin pigments) [23, 24, 25, 26]. Calculations of fundamental thermodynamic properties of aromatic sulfur compounds, such as molar enthalpies of formation and standard molar enthalpies of phase transitions, can be found in several quantum chemistry papers are given in Table 2 [27].

| Thiophene | Benzothiophene | Dibenzothiophene | 4,6-Dimethyldibenzothiophene |
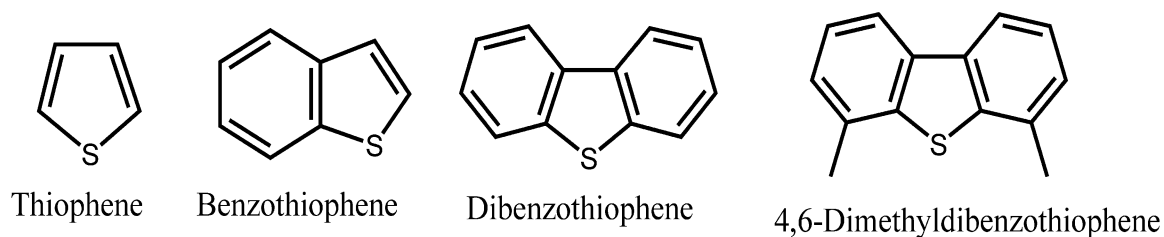
Figure 1: Aromatic sulfur compounds present in fuels

Table 2: Physical properties of some aromatic sulfur compounds

Aromatic sulfur compounds	Formula	Boiling point, K	Density, g/cm^3	Solubility in Tetradecane	Dipole moment, D
Thiophene (T)	C_4H_4S	357	1.051	Soluble	0.53
Benzothiophene (BT)	C_8H_6S	494	1.15	Soluble	3.04
Dibenzothiophene (DBT)	$C_{12}H_8S$	605	1.252	Soluble	0.79
4,6-dimethyl dibenzothiophene (4,6-DMDBT)	$C_{14}H_{12}S$	637.9	1.181	Soluble	Not available

1.3 Methods of Desulfurization of Liquid Fuels

There are several methods to remove sulfur compounds from fossil fuels such as gasoline, diesel, and jet fuels. Some of these methods have been well-investigated and are used industrially, e.g. conventional hydrodesulphurization (used on an industrial scale at refineries). However, hydrodesulfurization (HDS) is not effective enough for ultra-deep desulfurization of fuels containing large amounts of the large-ring aromatic sulfur compounds. Alternative methods need to be studied and developed using novel types of sorbents.

1.3.1 Hydrodesulphurization

Desulfurization of petroleum to produce clean liquid fuels such as gasoline or diesel via catalytic HDS is well known used in industry. Most of the sulfur compounds present in fossil fuel, thiols, thiolates, sulfoxides and sulfones, are removed by hydrodesulphurization at high temperature and pressure. The industrial method to remove aromatic sulfur compounds from fossil hydrocarbon fuels by catalytic HDS is (1) not effective in ultradeep removal of large-ring aromatic sulfur compounds below about 15 ppmw total sulfur, (2) not very selective for aromatic sulfur compounds versus other aromatic compounds, such as naphthalene, due to the similarity of large aromatic rings structure, (3) energy demanding and (4) not CO_2 neutral. Many alkyl-substituted aromatic sulfur compounds such as benzonaphthothiophenes and dibenzothiophenes, e.g 4,6-DMDBT are "refractory" (i.e., it is difficult to remove them by HDS process [28,29]. The mechanism of refractory behavior of large-ring aromatic sulfur compounds via HDS is a sterical hindrance effect [30]. Specifically, the two methyl groups in 4,6-DMDBT prevent the sulfur atom from accessing the catalytically active site.

1.3.2 Photooxidation

Heterogeneous photocatalysis has been utilized for environmental applications, such as purification of water and air via photocatalytic oxidation [31]. Recently, there has been a strong growth of interest towards photocatalysis such as photocatalytic water splitting and photocatalytic CO_2 reduction [32]. From a practical standpoint, heterogeneous photocatalysis of aromatic sulfur compounds is of relevance to petrochemistry [33], emerging "ultraclean" fuels for fuel cells, and environmental research and applications [31].

1.3.3 Oxidative Desulfurization

Among catalysis-based methods of removal of aromatic sulfur compounds, catalytic oxidation is of major interest. Oxidative desulfurization has been used particularly for diesel desulfurization. In this method, sulfur compounds are converted to oxidized sulfur species via oxidative chemicals such as HNO_3, NO/NO_2, and RuO_4. In contrast to HDS that produces H_2S, the oxidative desulfurization process removes oxidation products by solvent extraction. Oxidative desulfurization proceeds at mild conditions and does not need molecular hydrogen gas H_2 [34]. The major disadvantages of desulfurization via catalytic oxidation are the use of expensive chemicals, (organic peroxides and H_2O_2), the use of highly corrosive or oxidative liquid media, and the need to dispose of chemical waste [35].

1.3.4 Biodesulfurization

Another method for removing aromatic sulfur compounds from liquid fuels is biodesulfurization. Sulfur is a necessary element for some microorganisms to grow and sustain life [36]. So, microorganisms can be used to convert aromatic sulfur compounds into oxidized aromatic sulfur molecules which can be then removed by adsorption under ambient conditions. The biodesulfurization process has been used to remove sulfur compounds under mild conditions, via a non-invasive approach, and it has recently been applied to industrial desulfurization [37].

1.4 Adsorption of Aromatic Sulfur Compounds from Liquid Phase

Adsorption of aromatic sulfur compounds via an ion-exchange zeolite and a metal halide-impregnated carbon is a promising desulfurization method to remove sulfur

selectively from liquid fuels [38,39]. There are many specific advantages of using an adsorption process to remove sulfur from petroleum and gasoline. Firstly, the adsorption process can occur at ambient conditions (room temperature and atmospheric pressure), which make it a low cost process. Secondly, the adsorption process does not have to consume any oxygen and hydrogen. Many adsorbents such as zeolites (mesoporous materials) and activated carbon have been investigated for desulfurization. Ma and Yang have researched using an ion-exchanged zeolite and metal halide-impregnated carbon for desulfurization of liquid fuels [40]. These researchers showed that the adsorption capacity of metal halide-impregnated carbon for refractory aromatic sulfur compounds is higher than that of ion-exchanged zeolites. Kim *et al.* have analyzed metals such as Ni (deposited on silica gel), aluminum and activated carbon to remove refractory aromatic sulfur compounds and aromatic nitrogen compounds selectively [41]. This research also indicated that the adsorption capacity of metal halide-impregnated activated carbon is related to surface area, total pore volume, and Brunauer-Emmett-Teller (BET) surface area (which is directly proportional to adsorption capacity). These results are consistent with the microspore diameter and dimensions of both aromatic sulfur compounds and metal cations (Cu^+, Ni^{2+}, Zn^{2+}) which are of critical importance for adsorption of sulfur compounds, particularly aromatic compounds [40].

1.5 Metal-Organic Frameworks MOFs

Metal-Organic Frameworks (MOFs) are a new class of metal-organic polymers which are known for their very high adsorption capacity, particularly of hydrogen at moderate operation conditions. The structure of MOFs is formed by the metal site bound to the organic ligand thus forming three dimensional polymer networks, which are of

inorganic-organic hybrid type. Bonding occurs between metal ions and organic linkers, the latter acting as bridging ligands between the metal ions to compose a 3D structure. The number of possible structures of MOFs is virtually infinite due to the variety of available subclasses of MOFs [42, 43, 44, 45].

MOFs are promising materials for industrial usage such as for gas storage, separation, sensing, catalysis and adsorption of unwanted species [42, 43, 44]. MOFs have many great properties such as large pore volume, high BET surface area and high inner surface area (Table 3). Moreover, host-guest interaction of MOFs with substrate molecules makes MOFs very important for applications. Although investigation of MOFs for adsorption of aromatic sulfur compounds such as BT and DBT has been reported [46], industrial usage of MOFs as a sorbent has not occurred. One of the well-investigated MOFs is HKUST-1, also known as Basolite C300 Cu-MOF. Figure 2 shows the structure of Cu-MOF with formula $C_{18}H_6Cu_3O_{12}$. Grey balls indicate Carbon, red balls indicate Oxygen, and purple balls indicate Cu^{2+} [47]. Although the structure of Cu-MOF is well known, the detailed structure of its counterpart Fe-MOF is not known in detail.

Figure 2: Structure of Cu-MOF [47], see Supplementary Data (Figure S2)

Table 3: Literature data on surface area, pore size and pore volume of sorbent [46]

Adsorbent	BET surface area, m^2/g	Barrett-Joyner-Halenda (BJH) pore volume, cm^3/g	BJH pore size, nm
C300	1277	6.1	0.61
F300	854	6	0.6
Y-Zeolite	662	1.9	0.74

1.6 Adsorption of Aromatic Sulfur Compounds on MOFs

MOFs have been used as sorbents for many kinds of adsorbates. However, there is a limited number of publications on the adsorption of large organic molecules such as aromatic compounds. Recently, the adsorption of aromatic sulfur compounds on many MOFs has been investigated as a way to obtain low-sulfur liquid fuels. The adsorption on MOF sorbents, including HKUST-1, has been studied much less often in liquid phase, compared to adsorption in gas phase. The problem of the fast deactivation of the catalyst due to incomplete desorption of reaction products is well understood [48]. Regeneration of "spent" sorbent is of importance, since its efficiency determines the usable lifetime of the sorbent, operating costs and practical aspects of the scale-up of desulfurization process.

Adsorption isotherms and capacities of HKUST-1 have been reported for BT, DBT and 4,6-DMDBT; these isotherms and capacities were measured in an isooctane solvent at room temperature in batch experiments [49]. Isooctane (boiling point 99 °C) as component of such model fuels was apparently intended to model gasoline. For BT, at an

initial content of sulfur (present as an aromatic sulfur compound) of 1500 ppmw in this model fuel, the adsorption capacity reaches 25 g S/kg sorbent. For DBT, at an initial content of 1500 ppmw S in this model fuel, the capacity is 45 g S/kg sorbent, and for 4,6-DMDBT at 600 ppmw S in this model fuel, the capacity is 16 g S/kg sorbent. The regeneration of "spent" HKUST-1 sorbent after adsorption of BT, DBT and 4,6-DMDBT was achieved [48] via rinsing with isooctane for 24 hr. Adsorption capacity for "regenerated" HKUST-1 sorbent was not reported in these studies.

The adsorption isotherms and capacities of C300 Basolite MOF for BT, DBT and 4,6-DMDBT in isooctane (also known as 2,2,4-trimethylpentane) have also been reported [46]. The time for establishing adsorption equilibrium was chosen as 72 hours in all cases, although the kinetics of adsorption was not studied. The adsorption capacity and isotherms at 283-333 K were measured in separate experiments (one sample per one data point), and the adsorption capacity of the regenerated sorbent was not investigated. At an initial concentration of DBT of 1724 ppmw, the adsorption capacity was 45 g S/kg sorbent at 304 K. The adsorption capacity of BT was calculated to be 40 g/kg sorbent at 304 K, and for 4,6-DMDBT it was calculated to be 13 g/kg. "Spent" C300 MOF sorbent after adsorption of DBT was studied by XPS [46], and an oxidized form of sulfur S(VI) was found based on an XPS S2p peak at binding energy (BE) of 169.2 eV. A sulfone form of DBT was assumed to have formed upon adsorption of DBT onto C300 in air, i.e., a surface chemical reaction rather than reversible adsorption took place. Based on the XPS data above, one cannot expect to reuse regenerated C300 for adsorption, since DBT sulfone is not soluble in hydrocarbons. On the other hand, one should note that prior to XPS, the sample was handled in ambient air, so oxidation of the adsorption complex

might have taken place *before* XPS measurement. In addition, XPS spectroscopy *itself* can be destructive to the specimens, due to both X-ray and electron induced sample damage [50]. Therefore, in-situ, non-destructive methods need to be used with sample, particularly, without exposure to oxygen and humidity that strongly affects the adsorption properties of most MOFs.

Adsorption isotherms and capacities of C300 Basolite MOF for thiophene, BT, and DBT in isooctane [51] were also reported at 293-303 K. The time for establishing adsorption equilibrium was chosen as 24 hours, although the kinetics of adsorption was not studied. The adsorption capacity and isotherms were measured in separate experiments, and the adsorption capacity of regenerated sorbent was not investigated. At 293 K, using an initial concentration of 370 ppmw S, the adsorption capacity is 32 g S/kg for DBT, 81 g/kg for BT, and 28 g/kg for thiophene [51].

In all the studies discussed above, the hydrocarbon solvent was isooctane which is a model solvent for gasoline with a lower boiling point range, as compared to diesel fuel. Model solvents for diesel and oil would need to have a straight-chain alkane with a higher boiling point as a solvent. Adsorption studies on such model fuels have not been reported. Also, the adsorption capacities discussed above were reported either as g S/ kg MOF sorbent, or as mmol S/g sorbent. Therefore, it is not known whether adsorption complexes with distinct chemical stoichiometry are formed upon adsorption of aromatic sulfur compounds on HKUST-1 sorbent. Adsorption/desorption cycles for aromatic sulfur compounds in *liquid phase* were reported for zeolites [52]. In these studies, the "spent" sorbent needed to be separated by filtration after each adsorption cycle. So, the organic adsorbates would not be oxidized by ambient air [46]. Otherwise, a chemical

(surface) reaction would occur that would render the MOF sorbent not usable for the following adsorption. It would be useful to apply the experimental methods discussed above for quantitative studies of adsorption and desorption. In this case, desorption is (1) nondestructive, (2) proceeds back to the liquid phase of the adsorption medium, and (3) the adsorption capacity can be measured again *after* the cycle "adsorption/desorption".

1.7 Research Objective

The general objective of this research is to investigate adsorption and desorption of aromatic sulfur compounds on certain MOFs. One specific objective of this study is to investigate how the adsorption and desorption of aromatic sulfur compounds on MOFs depend upon temperature. Another specific objective is to learn about the mechanism of adsorption-desorption of aromatic sulfur compounds on MOFs.

These goals will be accomplished using the following approaches. We will investigate:

1) if any chemical reaction takes place during the interaction of aromatic sulfur compounds with MOFs.

2) the dependence of adsorption capacity upon temperature.

3) the stoichiometry of adsorption complexes formed by molecules of aromatic sulfur compounds with MOFs.

4) the kind of binding in adsorption complexes using fluorescence spectroscopy.

Chapter 2: Experimental

2.1 Aromatic sulfur Compounds

Thiophene, BT, DBT and 4,6-DMDBT and n-tetradecane were obtained from Sigma Aldrich and used as received. The MOFs Basolite C300 and F300 were bought from Sigma Aldrich and were activated prior to adsorption tests.

2.2 Model Fuels

Model liquid fuels containing thiophene, BT, DBT, or 4,6-DMDBT were prepared by dissolving the respective aromatic sulfur compounds in tetradecane at an initial concentration of 0.033 M (for thiophene, BT, and DBT), and at 0.022 M (for 4,6-DMDBT). These concentrations were chosen (1) due to the fact that they are close to maximum solubility of aromatic sulfur compounds in tetradecane and (2) in order to achieve the maximum adsorption capacity on Cu-MOF. Also, such concentrations are close to those found in commercial high-sulfur heating oils, jet fuels [5] and certain refinery naphthas. Tetradecane was used because of its high boiling point (253 °C) and its similarity to the aliphatic hydrocarbons found in diesel fuel.

2.3 Activation of MOFs before Adsorption

MOFs need to be activated prior to adsorption experiments because MOFs readily adsorb water under ambient conditions. Activation of MOFs includes desorption of water, oxygen and other volatile impurities present in the MOF since their synthesis. Activation of Cu-MOF was performed via heating at 150 °C for 24 hrs in a vacuum of $< 1 \times 10^{-4}$ Torr. This process was based on a previously reported process for activating Cu-MOF [47].
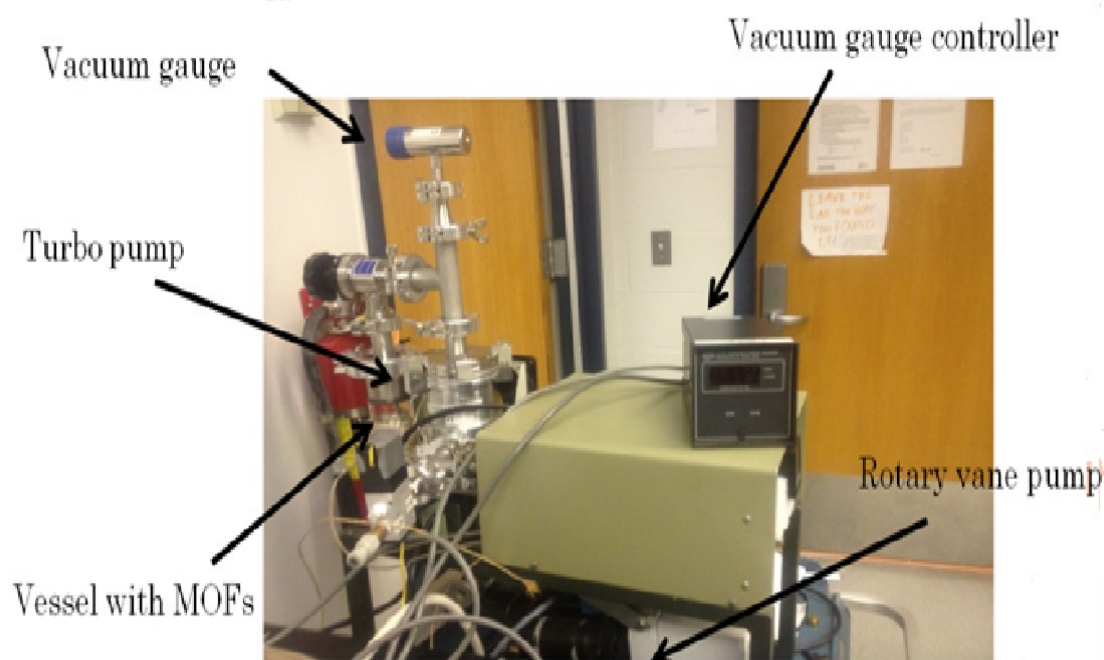
Figure 3: Apparatus for activation of MOFs

Figure 3 shows our homemade apparatus for activation of MOFs. This setup contains one oil roughing pump and turbo pump. The vacuum gauge controller shows current pressure any time. Up to four glass of quartz vessels with MOFs can be loaded into the activation setup at the same time.

2.4 UV/Vis Spectrum and Calibration Curve of Aromatic Sulfur Compounds

The UV/VIS spectrometer (model Cary Biorad-50) was used to measure UV/VIS spectra of solutions of aromatic sulfur compounds. This UV/VIS spectrometer was also used to construct a calibration curve and determine the equilibrium concentration of the aromatic sulfur compound in solution before or after adsorption. Before constructing the calibration curve, the solutions were diluted to avoid instrument signal saturation and to keep the absorbance between 0 and 1 absorbance unit.

2.5 Adsorption at Constant Temperature

Figure 4: Apparatus of adsorption/desorption connected to the shaker

The apparatus for adsorption/desorption was built by us. Its two main components, shaker and heater, are connected to each other as shown in Figure 4. The thermocouple is connected to the vessel containing the suspension of model fuel and MOF to determine the temperature at any given time. Four adsorption vessels with suspension can be loaded into the apparatus at the same time. A heat insulating cover (not shown in Figure 4) is a part of the apparatus to create isothermic conditions of adsorption experiments.
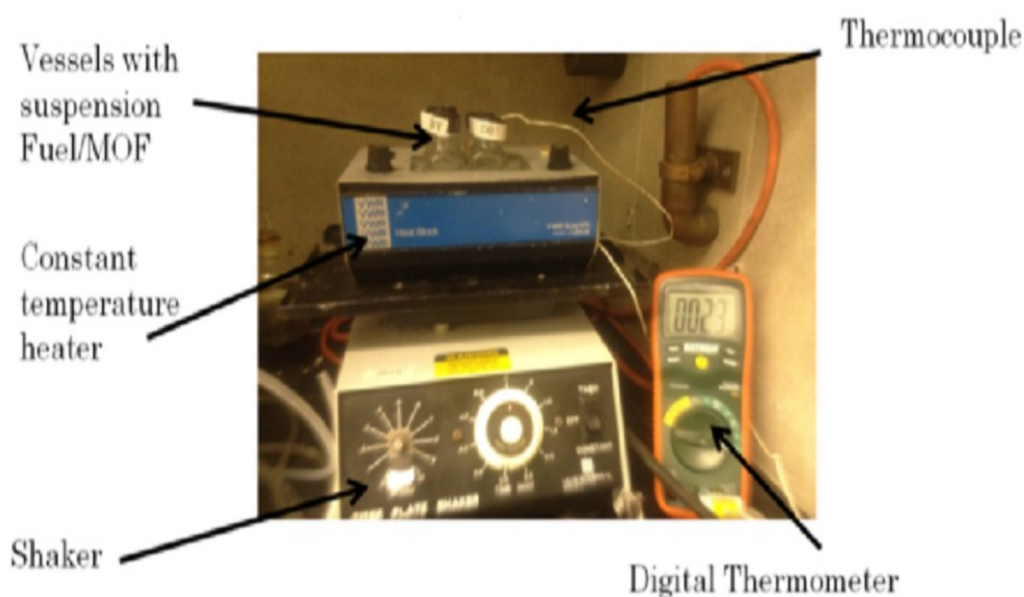
We used Cu-MOF for adsorption after its outgassing. After outgassing, we mixed 0.30 g Cu-MOF with 50 ml of 0.033 M solution of either thiophene, BT, DBT. Alternatively, we used 50 ml 0.022 M solution of 4, 6-DMDBT. Our solutions were placed onto the shaker attached to the heater for adsorption-desorption experiment at constant temperature. Adsorption was allowed to proceed for up to 11 hours at room temperature (298 K), under continuous shaking.

Periodically, we collected a small aliquot (ca. 0.2 ml) of suspension, and centrifuged it to obtain a clear supernatant. We analyzed the clear supernatant by the HPLC-UV and the UV-Vis spectroscopy to determine the chemical composition of the fuel after adsorption and the remaining concentration of aromatic sulfur compounds.

At constant temperature, we also determined the kinetics of the adsorption of DBT with Cu-MOF from 0.033 M, 0.00033 M and 0.000033 M 25 ml solutions by collecting 0.6 ml aliquots 9 times (1, 2, 3, 4, 5, 6, 8, 10 and 24 hours).

2.6 Adsorption at Variable Temperature

We used Cu-MOF for adsorption at various temperatures after its outgassing. We mixed 0.30 g Cu-MOF with 50 ml of 0.033 M solution of either thiophene, BT, or DBT, or with 50 ml 0.022 M solution of 4,6-DMDBT. Our solutions were placed onto the shaker connected to the heater for adsorption-desorption process.

For adsorption at variable temperatures, the setup was additionally equipped with a Proportional Integral Derivative (PID) temperature controller from Auber Instruments, Inc. This controller was programmed by us to achieve variable temperatures as below, following manufacturer's instructions. The whole experiment was conducted while continuously shaking the specimen. At constant temperature, we waited 11 hours at 298 K to reach thermodynamic equilibrium, and then a 0.2 ml of suspension was collected for analysis. The rest of the sample was heated up to 348 K in the course of 1 hour. After allowing a period of 11 hours for the system to reach equilibrium at 348 K, a 0.2 ml sample suspension was collected again for analysis. Next, the temperature was further increased to 388 K over the course of 1 hour. After allowing a period of 11 hours for the system to reach thermodynamic equilibrium at 388 K, a 0.2 ml of suspension was collected again for analysis. Finally, the rest of the sample was allowed to spontaneously cool into 298 K (with the PID temperature controller turned off), and sampling and analysis was repeated after reaching equilibrium at 298 K. All these processes are shown in Figure 5. In all experiments, we assume (except for systematic error due to sampling of small volumes as above) a constant volume of liquid phase, a constant mass of MOF, and that mass balance is preserved. Mass balance in our (liquid-solid) adsorption system is

preserved at 298-388 K, since all substances used (except thiophene) have a negligibly low vapor pressure in this temperature range (due to having high boiling points).

The procedure for the analysis of the collected sample was as follows. We centrifuged the collected aliquot (ca. 0.2 ml) of suspension to obtain a clear supernatant. We analyzed the clear supernatant by HPLC-UV and UV-Vis spectroscopy to determine the chemical composition of fuel after adsorption, and the remaining concentration of aromatic sulfur compounds. Each adsorption experiment at variable temperature was repeated at least twice.
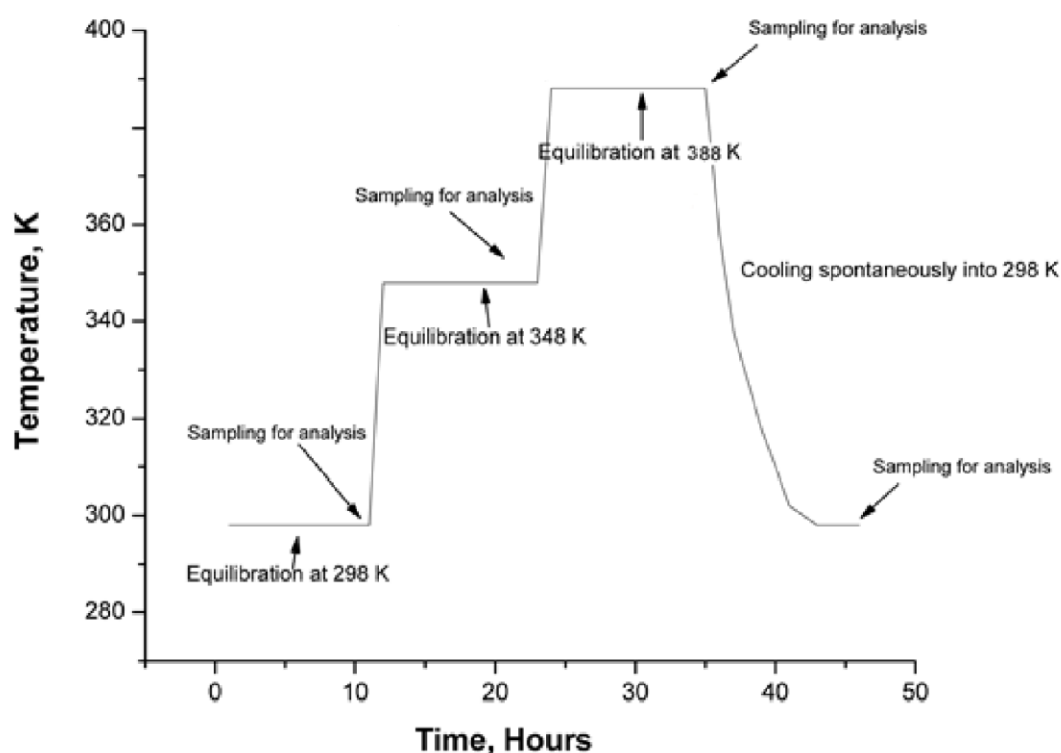

Figure 5: Sequence of heating and sampling for analysis

2.7 Chemical Analysis by HPLC-UV (High-Performance Liquid Chromatography)

To determine if any molecular products were produced from aromatic sulfur compounds under conditions of adsorption, we used an HPLC instrument (Model Gold from Beckman Coulter). This instrument is equipped with model 168 UV-Vis detector and C18 5-µm column. The eluent used was a mixture of 25 % vol. water and 75 % vol. acetonitrile. UV-Vis detection was monitored at λ=327 nm for DBT, and at λ= 299 nm for BT (see chapter 3 for an explanation of why these wavelength were chosen). Supernatant solutions were injected directly to the HPLC loop. The injection volume was 5 µL, and the flow rate was 0.8 mL/min.

2.8 Fluorescence Spectra of MOFs and Aromatic Sulfur Compounds

Fluorescence spectroscopy was used to detect the interaction between MOFs and aromatic sulfur compounds. The fluorescence spectrometer (Cary Eclipse) was equipped with standard fluorescence cell made of quartz. The slit widths were 5 nm for both emission and excitation.

2.9 Quantum Mechanical Calculations of Structure of Representative Aromatic Sulfur Compound

In this computational research, we examined the bond lengths, bond angles, UV/VIS spectra and the vibrational spectra of dibenzothiophene using the Gaussian view™ and Gaussian program. Our methodology was to use the Gaussian ™ program to determine the structure of the molecular compound, specifically, the UV/VIS spectra and the vibrational spectra of the molecule. The VSEPR theory was used to comprehend the

orbital nature of molecular compounds, and Schrodinger's equation was used for the calculation of the vibrational frequencies using various basis sets.

Our experiment was performed using the Gaussian software, which is a software package for use in computational chemistry. Gaussian allows us to calculate electronic structure and spectra of molecules and atoms. We performed our experiments on a computer running on Linux. We used GaussView 5.0 which is the graphical user interface to the Gaussian program. We ran several calculations. For geometry optimization of dibenzothiophene (DBT) $C_{12}H_8S$, we used Hartree-Fock level of the theory with the standard 6-311** basis set, for the IR spectra of DBT, we used DFT (B3LYP) level of theory using the standard 6-311G** basis set, and for the UV/VIS spectra of DBT, we applied TD-DFT (B3LYP) level of theory using the standard 6-311G** basis set.

Chapter 3: Results and Discussion

3.1 UV/Vis Spectra of Aromatic Sulfur Compounds and UV/Vis Calibration Curves
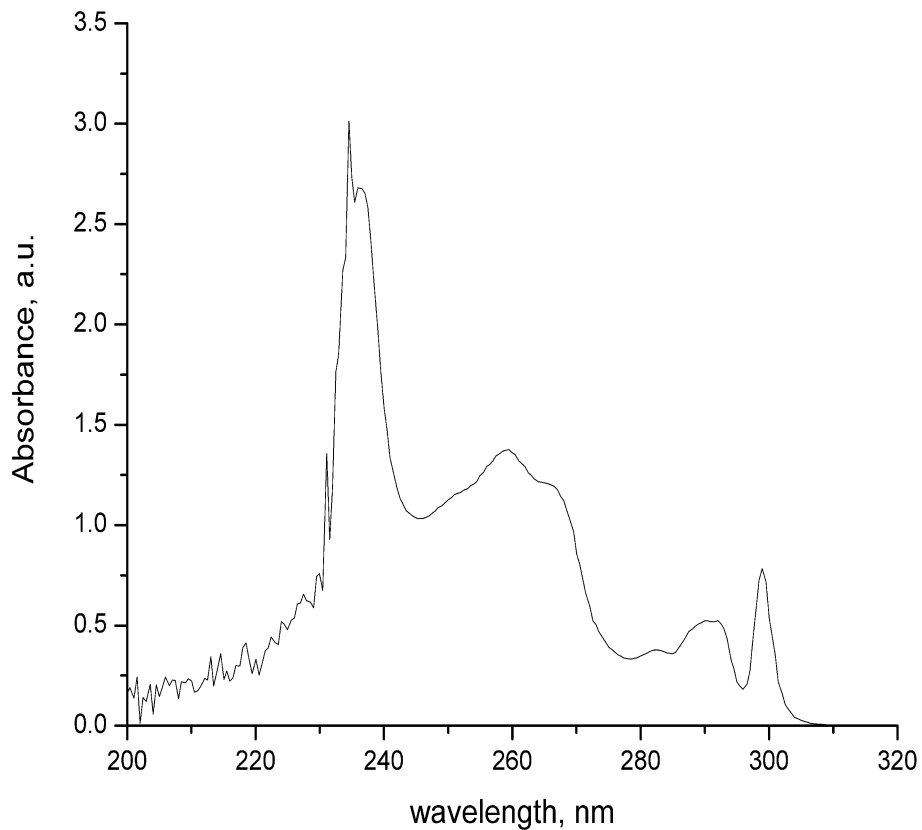
Figure 6: UV/VIS spectrum of the solution of Benzothiophene in n-$C_{14}H_{30}$

Peak identification for BT in tetradecane was conducted after using standards. As seen in the UV/VIS spectrum of solution of benzothiophene in Figure 6, BT gives a distinct narrow peak at 299 nm.
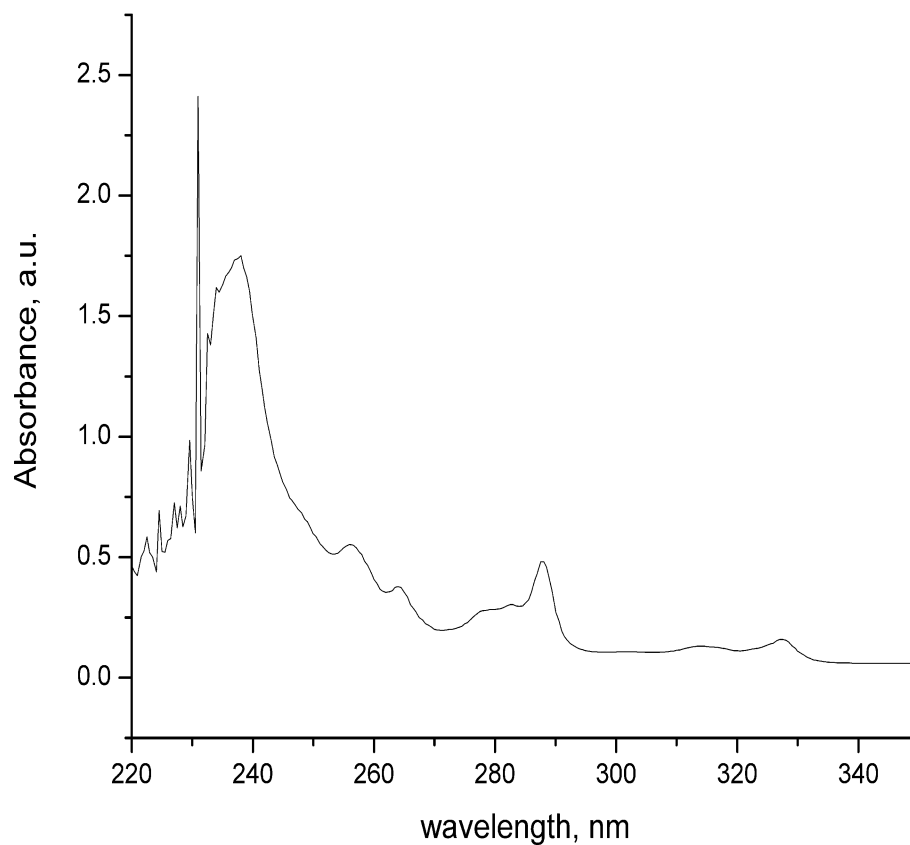
Figure 7: UV/VIS spectrum of the solution of Dibenzothiophene in n-$C_{14}H_{30}$

Peak identification for the solution of DBT in tetradecane was conducted using standards, and by comparison with spectrum reported in the literature [53]. The UV/VIS spectrum of Dibenzothiophene in Figure 7 shows that DBT gives a distinct small broad peak at 327 nm.
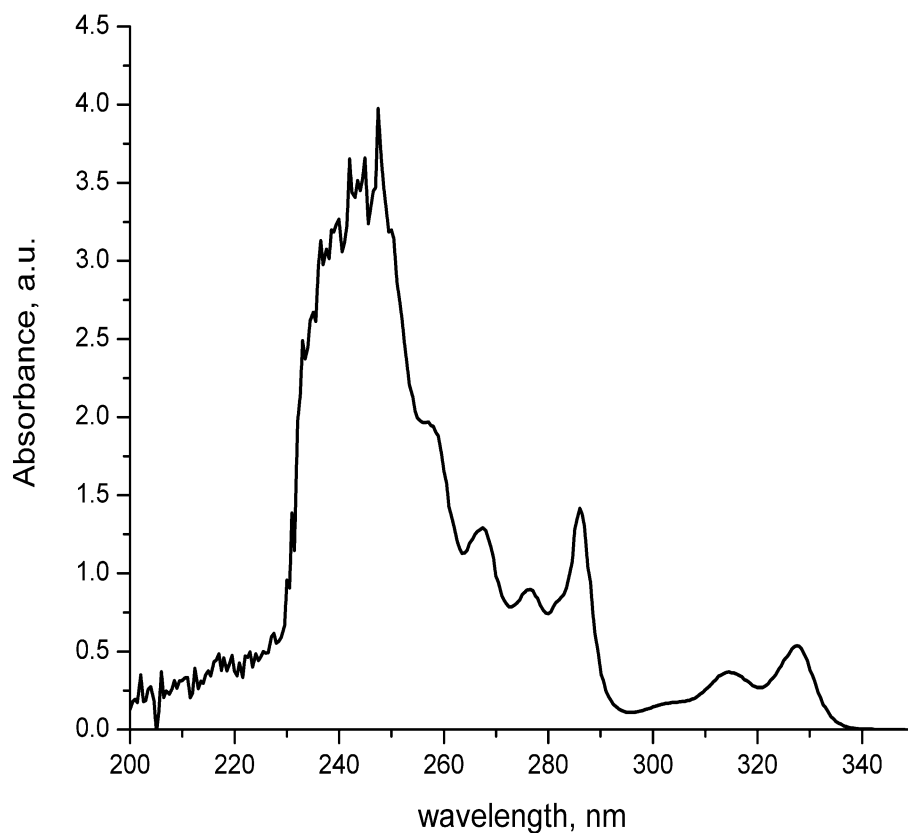
Figure 8: UV/VIS spectrum of the solution of 4,6-Dimethyldibenzothiophene in n-$C_{14}H_{30}$

The UV/VIS spectrum of 4,6-Dimethyldibenzothiophene in Figure 8 shows that, 4,6-DMDBT gives a well-defined peak at 327 nm. We note that UV-Vis absorption spectrum of 4,6-DMDBT resembles the one of DBT. This is due to the structural similarity between two molecules: the only difference is the presence of methyl substituent groups in the ring.
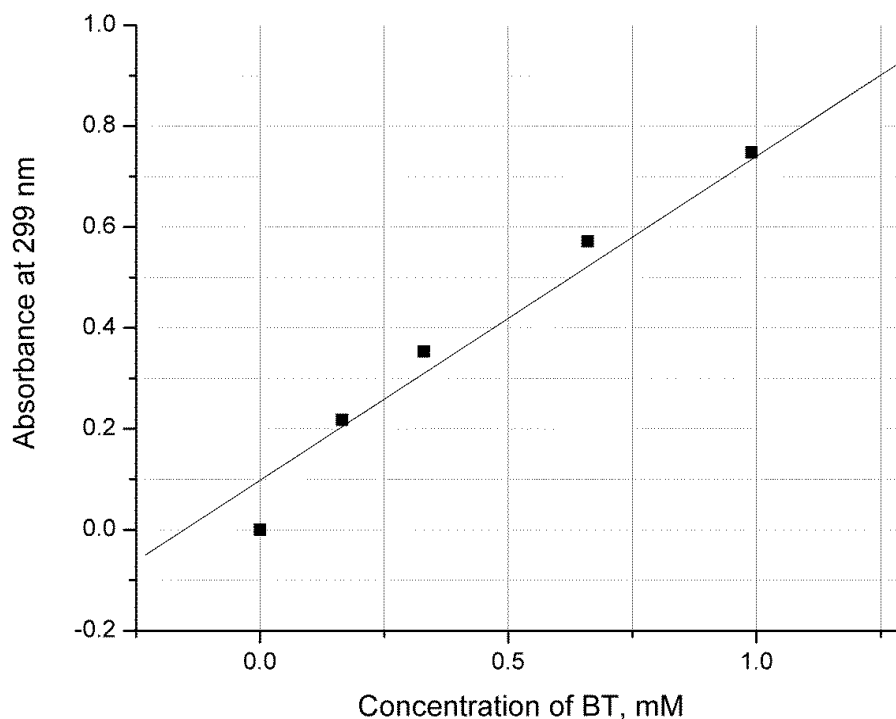
Figure 9: Calibration curve for quantitative determination of BT by UV/VIS spectroscopy

We have determined the UV-Vis absorption calibration curve for diluted solutions of BT at wavelength λ=299 nm (which is a maximum distinct absorption wavelength for BT shown in Figure 6). The graph is essentially linear within the range of concentrations 0 – 1 mM (Figure 9).

For the solution of 4, 6-DMDBT, its UV-Vis calibration curve as measured at λ=327 nm is shown in Figure 10. The graph is essentially linear within the range of concentrations 0–1 mM. For other aromatic sulfur compounds studied (thiophene and DBT), the calibration curves are linear (see Supplementary data).
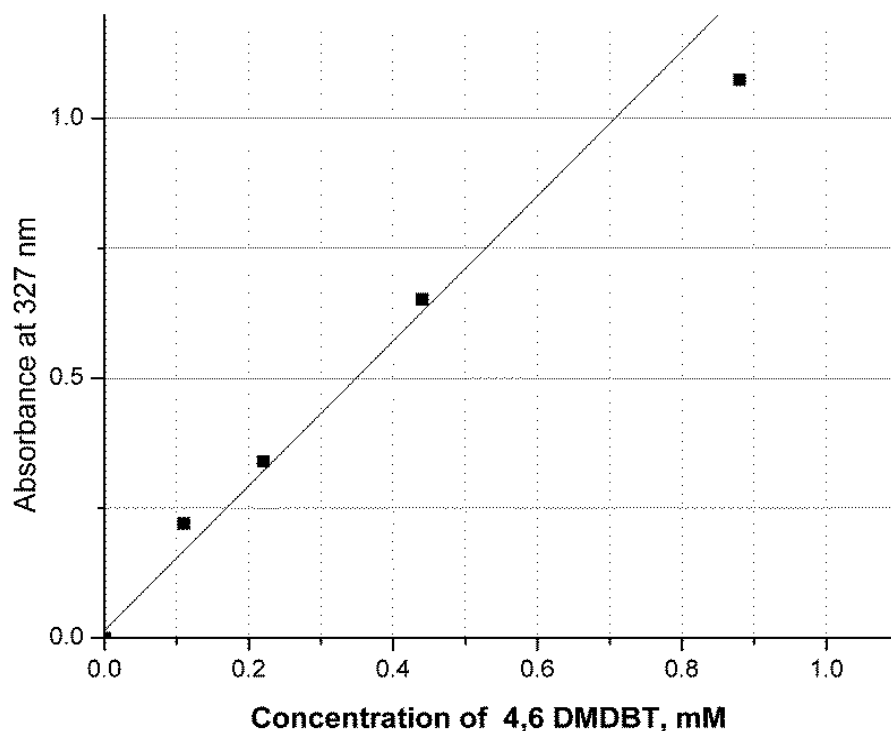
Figure 10: Calibration curve for quantitative determination of 4,6-DMDBT by UV/VIS

spectroscopy

3.2 Chemical Composition of Model Fuels by HPLC-UV after Adsorption

It was determined using HPLC-UV that aromatic sulfur compounds do not react

with MOFs during the adsorption desorption experiments. Specifically, the HPLC-UV

data indicate that there are no molecular products produced from BT (Figure 12) or DBT

mixed with MOF in the liquid phase.
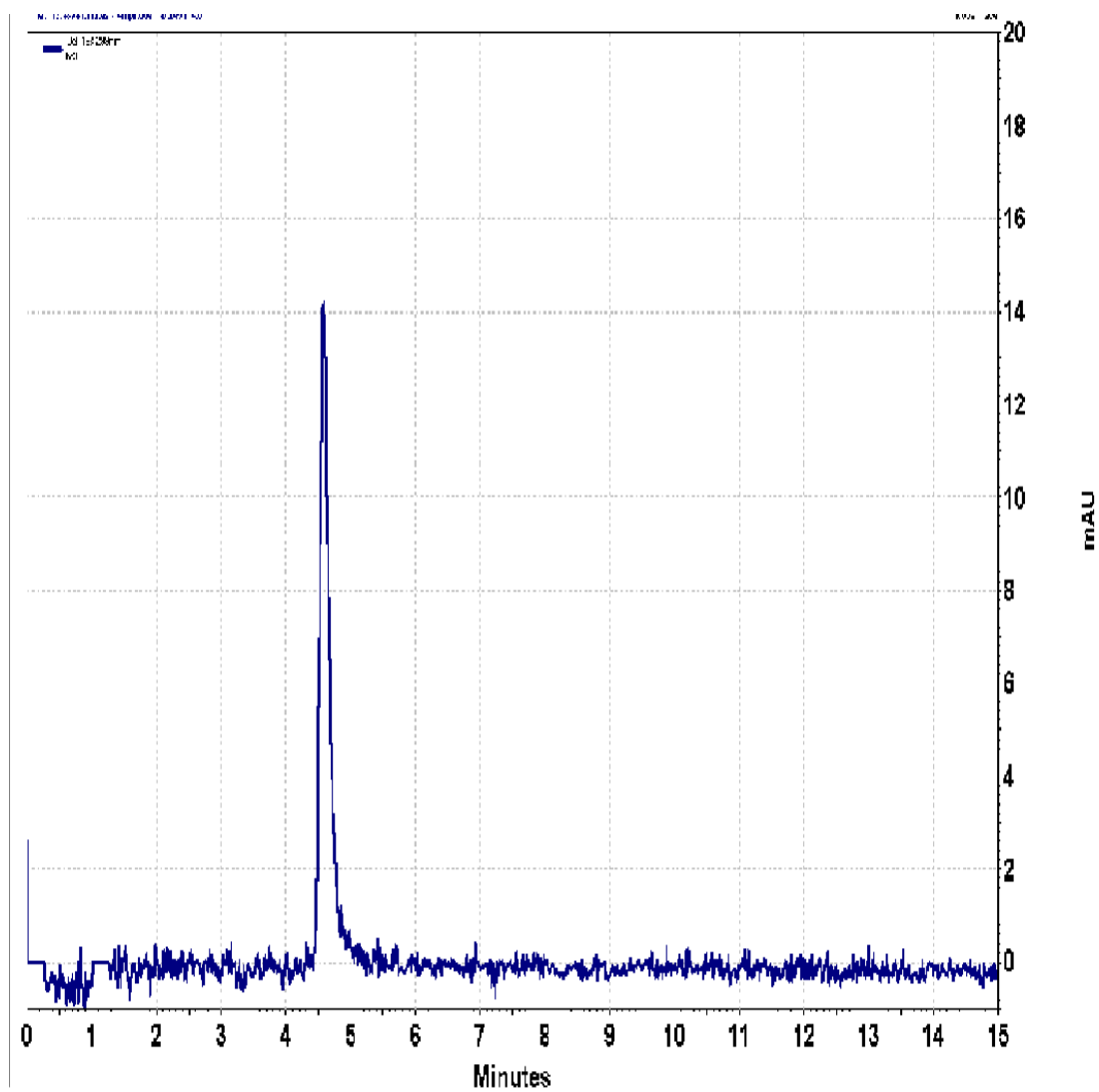
Figure 11: HPLC-UV time-dependent optical chromatogram of BT at 299 nm

Figure 11 shows the HPLC-UV time-dependent optical chromatogram for BT in $C_{14}H_{30}$ after adsorption/desorption on Cu-MOF. The only peak at a retention time about 4.6 min. belongs to BT as shown by injection of the BT standard.
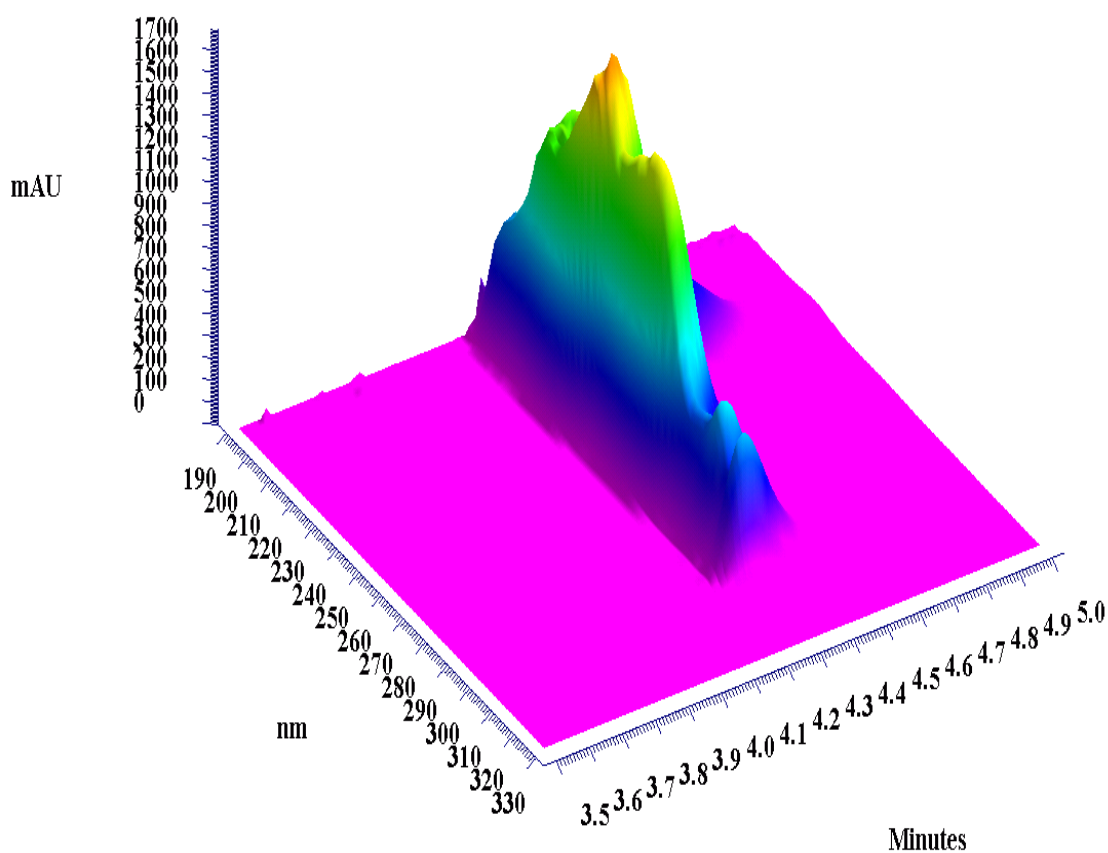
Figure 12: HPLC-UV time-absorbance 3D chromatogram of BT in $C_{14}H_{30}$

Figure 12 shows the HPLC-UV time-absorbance 3D chromatogram for BT in $C_{14}H_{30}$ after adsorption/desorption on Cu-MOF. The only peak at retention time about 4.6 min belongs to BT as shown by the injection of the BT standard.
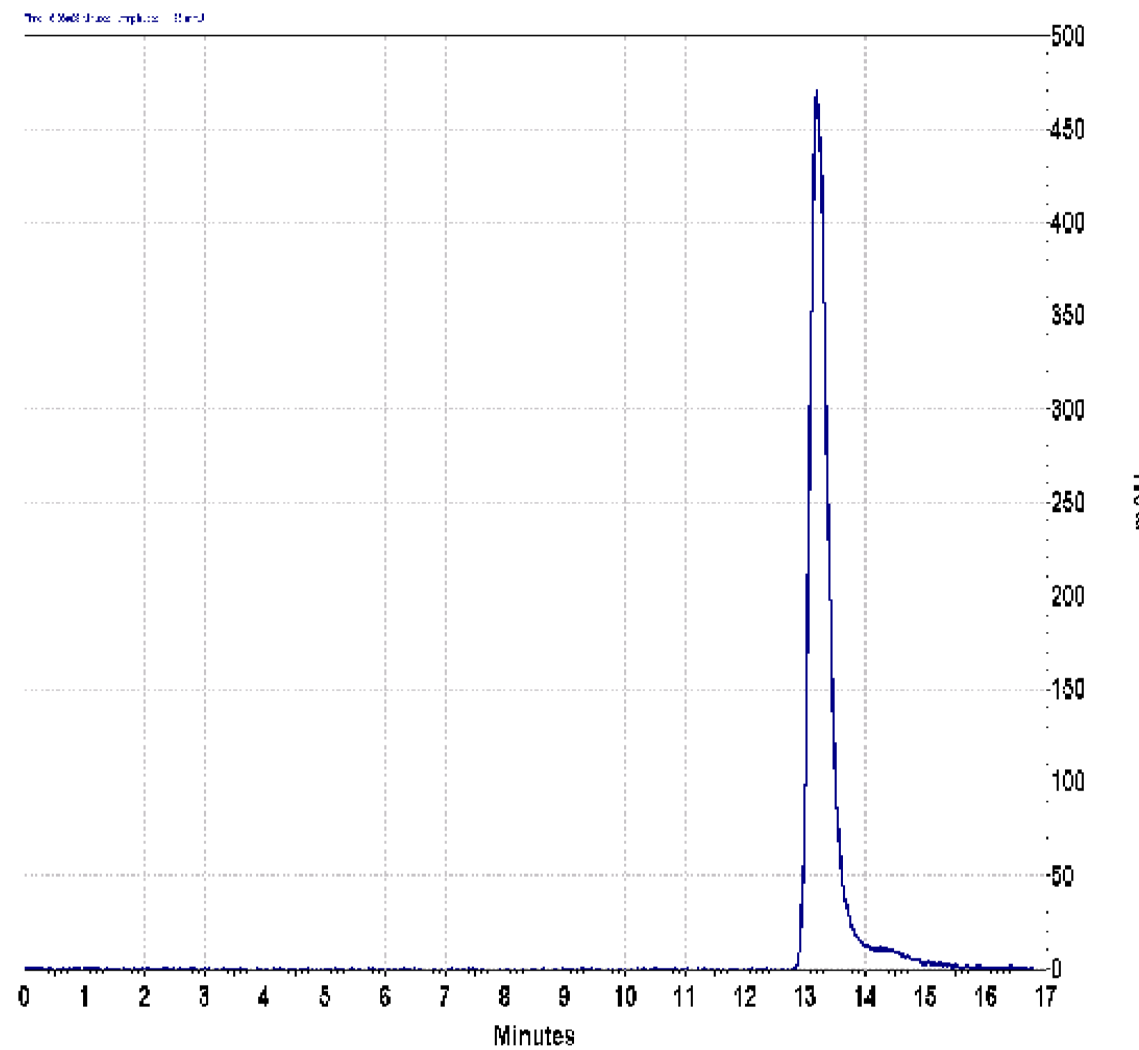
Figure 13: HPLC-UV time-dependent optical chromatogram of DBT at 326 nm

The HPLC-UV time-dependent optical chromatogram for DBT in $C_{14}H_{30}$ after adsorption/desorption on Cu-MOF can be seen in Figure 13. The only peak at retention time about 13.5 min. belongs to DBT as shown by the injection of the DBT standard.
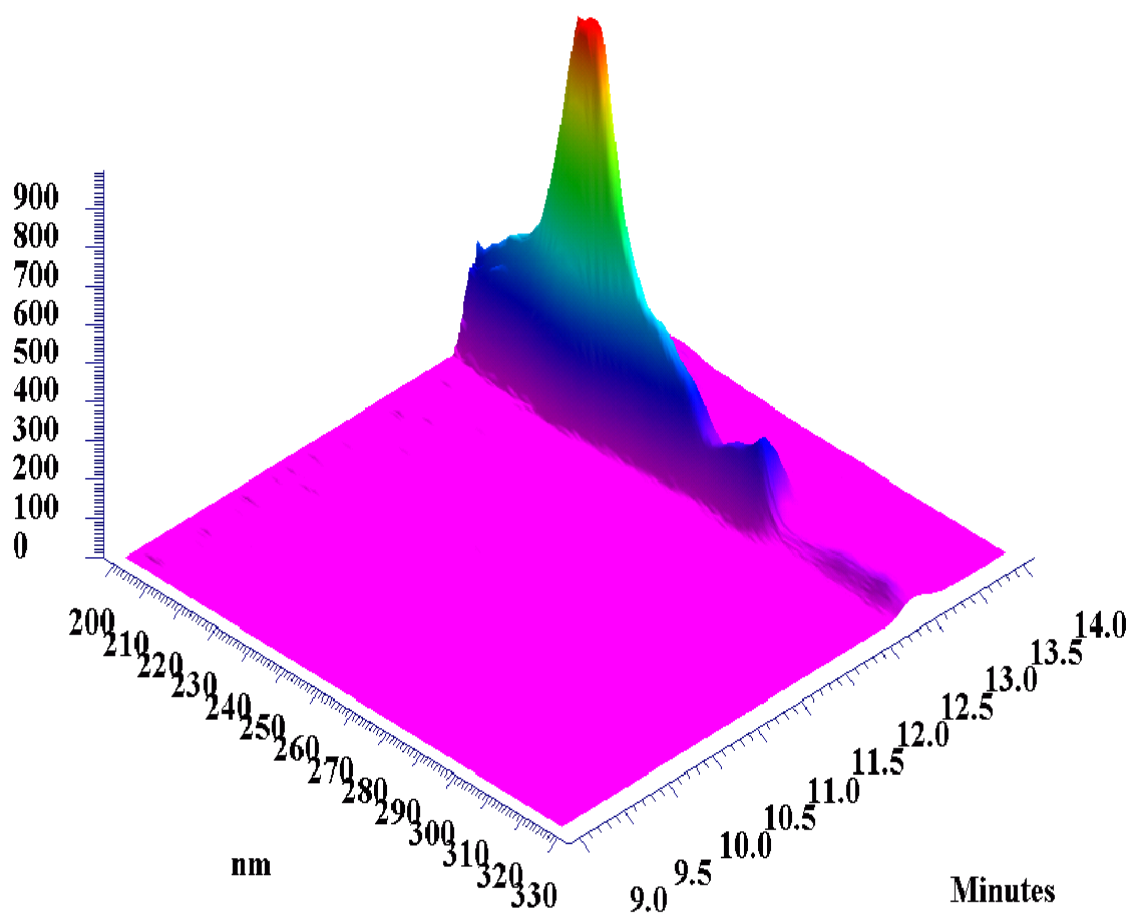
Figure 14: HPLC-UV time-absorbance 3D chromatogram of DBT in $C_{14}H_{30}$

Figure 14 shows the 3D HPLC-UV time-absorbance 3D chromatogram for DBT in $C_{14}H_{30}$ after adsorption/desorption on Cu-MOF. The only peak at retention time about 14 min belongs to DBT as shown by the injection of the DBT standard. The 3D form graphic of DBT was gathered after the adsorption/desorption process of DBT on Cu-MOF, and the whole trace was compared with a standard of DBT.

3.3 Kinetics of Adsorption at Constant Temperature

For the 0.000033 M DBT with Cu-MOF experiment, UV/VIS could not be used to measure the kinetics of adsorption; there was too low a concentration of DBT and too low an optical absorbance. For the 0.033M solution of DBT with Cu-MOF experiment, the adsorption kinetics is more complicated than the first order rate law, as found by a standard non-linear regression analysis.

We used an optical absorbance-adsorption time graph (Figure 15) directly, due to the optical absorbance of the solution of aromatic sulfur compound being proportional to its molar concentration as shown in Figures 9 and 10. This is explained by Beer-Lambert law, $A=\varepsilon bc$. In this formula, A is absorbance, ε is molar absorptivity and c is the sample concentration. The adsorption of DBT on Cu-MOF was found to be completed within about 5 hours (Figure 15).
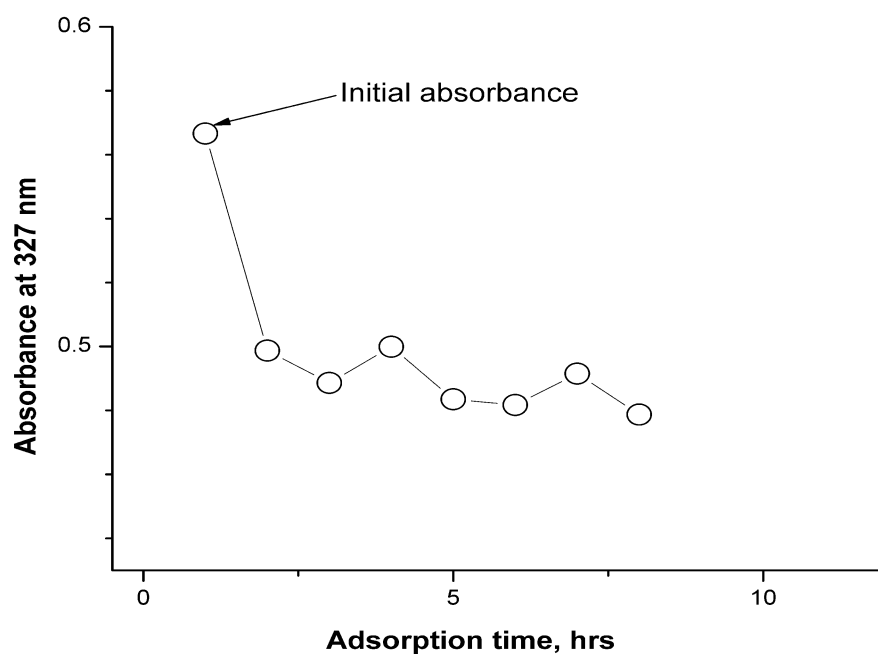
Figure 15: Kinetics of adsorption of DBT on Cu-MOF at 298 K

3.4 Temperature-Programmed Adsorption/Desorption of Aromatic Sulfur Compounds on MOF
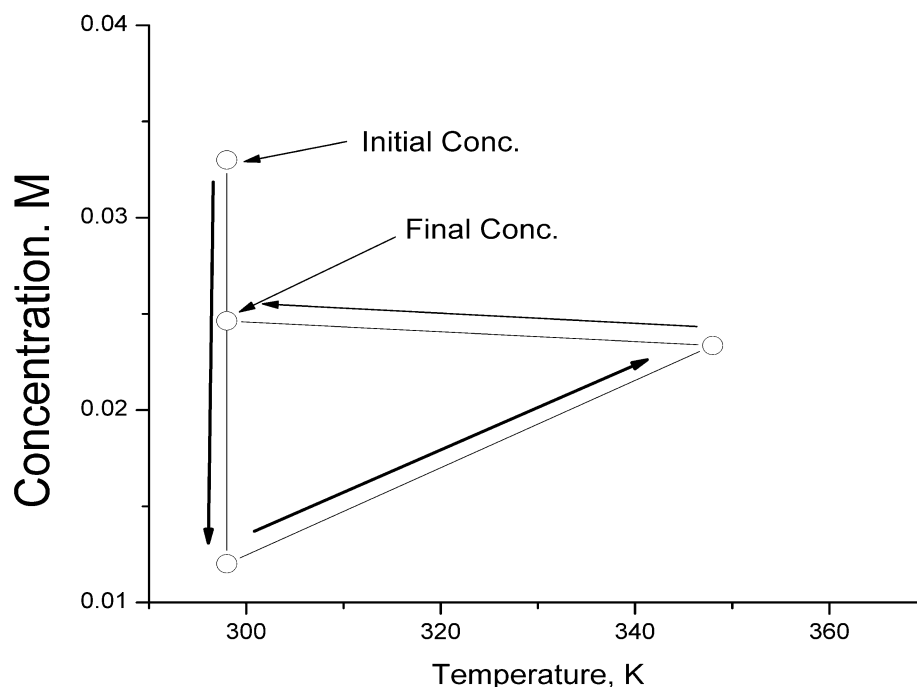
Figure 16: Adsorption/desorption cycle of Thiophene

Figure 16 shows that the initial molar concentration of thiophene in solution decreases from 0.033 M to 0.012 M upon adsorption at 298 K, then increases to 0.023 M upon heating up to 348 K. This finding indicates that thiophene partially desorbs from Cu-MOF when heated to 348 K. This temperature is close to the boiling point of thiophene (component of model fuels used by us), so we believe that some loss of thiophene occurs. Therefore, the final molar concentration of thiophene at 0.025 M observed should be treated with caution, since mass balance in adsorption experiment of thiophene was not maintained. Nevertheless, the observed desorption of thiophene from

Cu-MOF when heated to 348 K suggests that there is a reversible adsorption, rather than irreversible adsorption of thiophene on Cu-MOF.
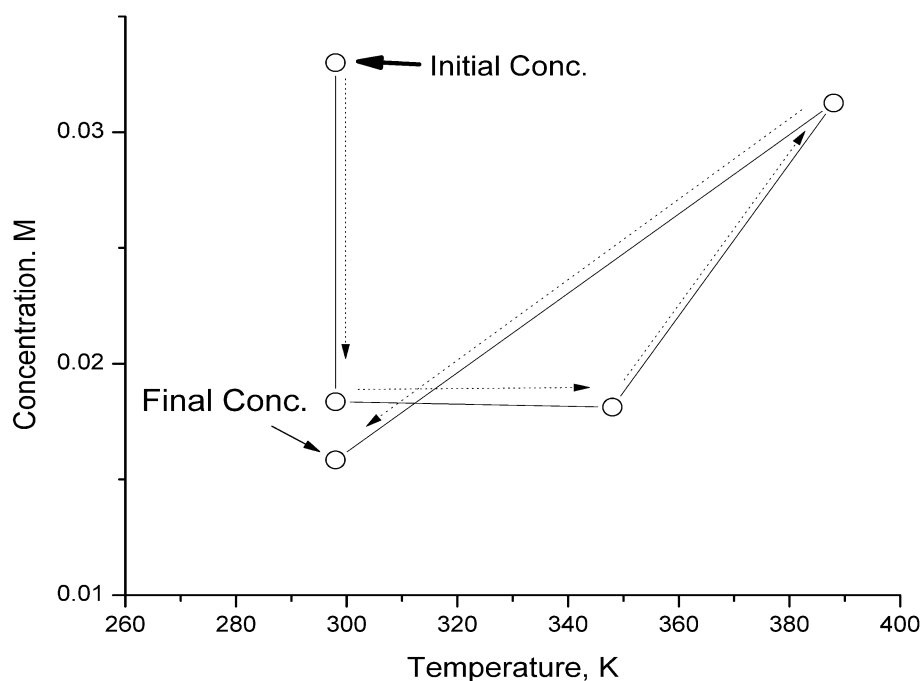
Figure 17: Adsorption/desorption cycle of BT

Figure 17 shows that the initial molar concentration of BT in solution decreases from 0.033 M to 0.018 M upon adsorption on Cu-MOF at 298 K. Upon heating to 348 K, the concentration of BT in the liquid phase remains about the same. However, after further heating to 388 K, the concentration of BT in the liquid phase significantly increases to about 0.032 M. Namely, nearly complete desorption of BT from Cu-MOF occurs at 388 K.

Upon subsequent cooling to 298 K, BT adsorbs back on Cu-MOF, with its remaining concentration in liquid being 0.018 M. We can make two conclusions: (1) adsorption is reversible, and (2) the Cu-MOF sorbent can be, potentially, re-used again after one cycle adsorption/desorption, since it provides nearly the same [BT] in liquid phase after heating as it did before heating.
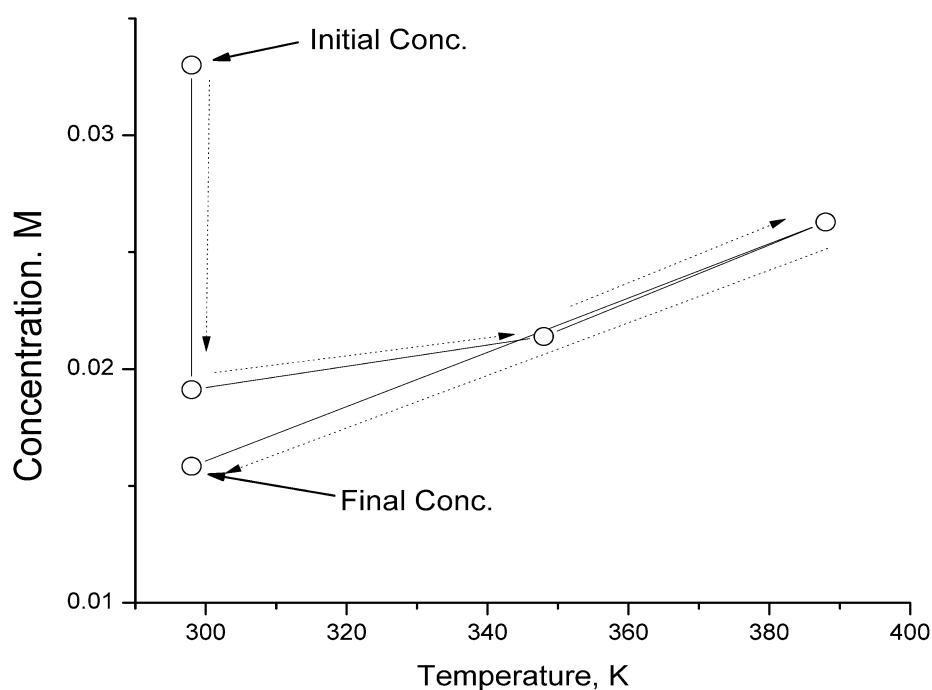
Figure 18 : Adsorption/desorption cycle of DBT

Figure 18 shows the concentration of DBT in the liquid phase after adsorption on Cu-MOF. After adsorption at 298 K, [DBT] decreases due to adsorption. At higher temperatures of 348 and 388 K, an increase of [DBT] in solution occurs. However, unlike the case of BT (Figure 18), desorption of DBT from Cu-MOF to liquid phase is not complete even at 388 K. After cooling the suspension to 298 K, [DBT] decreases, and

remains somewhat lower that [DBT] after adsorption at 298 K. Thus, Cu-MOF may be used as a re-usable adsorbent by arranging appropriate adsorption-desorption temperature programming.
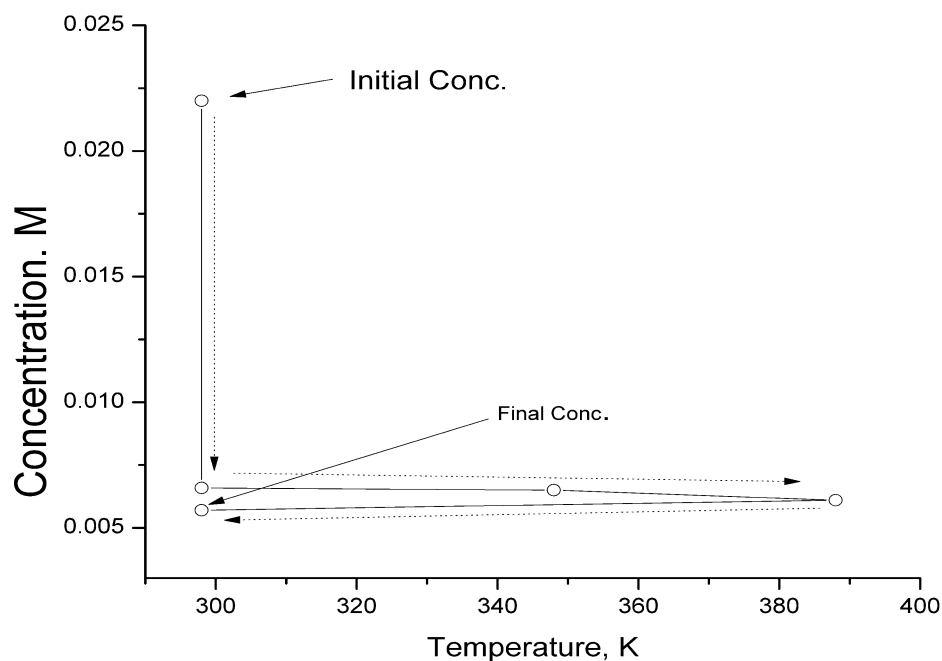
Figure 19 : Adsorption/desorption cycle of 4,6-DMDBT

Figure 19 shows the change in molar concentration of 4,6-DMDBT in the liquid phase following adsorption on Cu-MOF at variable temperature. After adsorption at 298 K, [4,6-DMDBT] decreases to 0.006 M and remains the same, regardless of the increase in temperature up to 388 K, as well as after the subsequent cooling to 298 K. Since the adsorbed amount of 4,6-DMDBT does not depend upon temperature, we conclude that (1) since 4,6-DMDBT is adsorbed on Cu-MOF at 298 K, and does not desorb even at 388

K, adsorption is irreversible, and (2) the Cu-MOF sorbent cannot be, potentially, re-used after one cycle adsorption/desorption, unless conditions for desorption can be found.
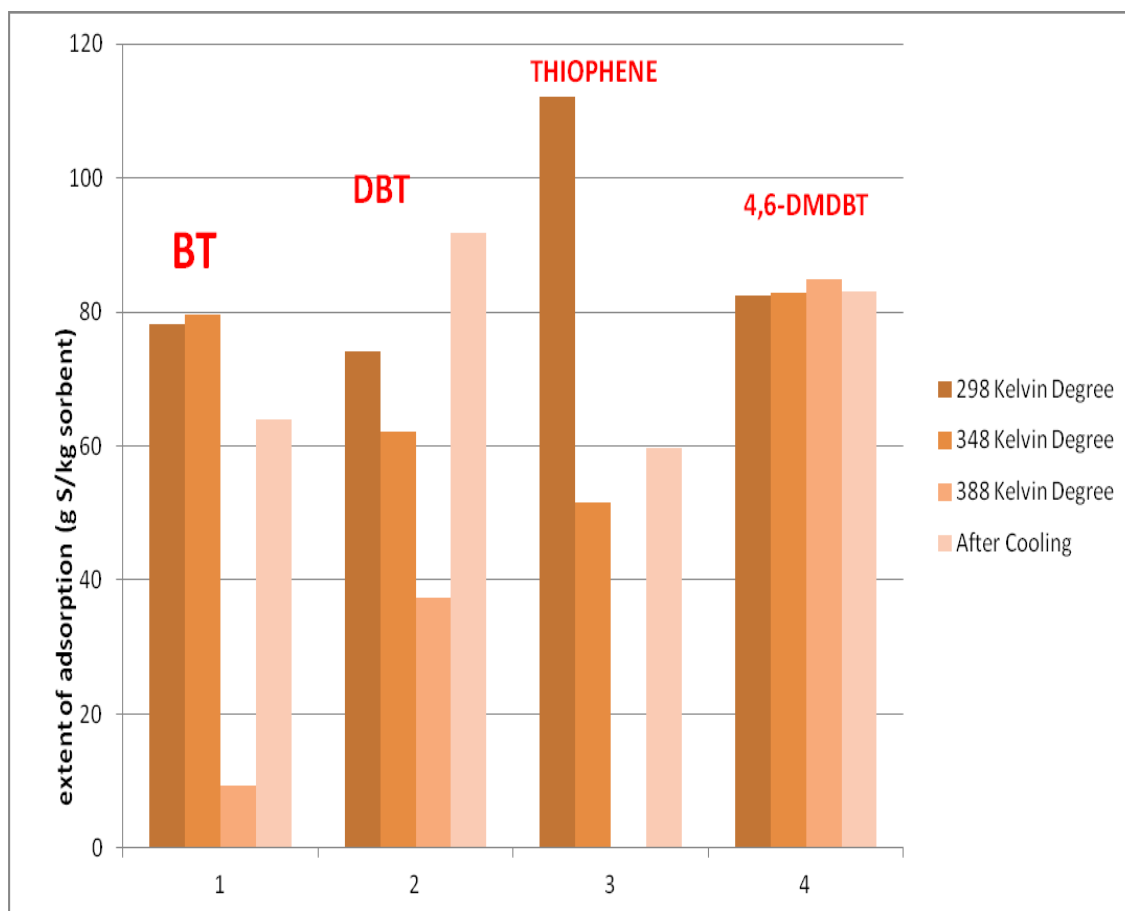
Figure 20 : Extent of sulfur compounds adsorption at equilibrium at 298, 348, 388 K.

Figure 20 shows the calculated adsorption capacity of the Cu-MOF versus BT, DBT, thiophene and 4,6-DMDBT in tetradecane as solvent, as calculated from the remaining molar concentrations in aliquots obtained at 298 K, 348 K, and 388 K. These aliquots were cooled back to 298 K prior to analysis. We found different adsorption capacities of C300 for different aromatic sulfur compounds.

As is indicated in Figure 20, the adsorption capacity of Cu-MOF towards BT is as high as 78.23 g S/kg sorbent at 298 K. When the temperature increases by 50 K to 348 K, the adsorption capacity of Cu-MOF remains about the same at 79.52 g S/kg sorbent. After heating up an additional 40 K, the adsorption capacity drastically drops down to 9.29 g S/kg sorbent. Finally, after cooling the suspension "MOF/model fuel" spontaneously (for almost 2 hours), the adsorption capacity reaches 63.69 g S/kg sorbent. Those results show that the adsorption capacity of Cu-MOF is about the same before and after adsorption, and therefore, Cu-MOF can be used as a reversible adsorbent by arranging a correct adsorption-desorption temperature program.

For DBT, (as shown in Figure 20), the adsorption capacity of Cu-MOF towards DBT is as high as 74.16 g S/kg sorbent. When the adsorption temperature increases by 50 K, adsorption capacity becomes lower at 62.04 g S/kg sorbent. At further heating up to 388 K, desorption occurs, with capacity going down to 37.33 g S/kg sorbent. Lastly, by cooling our solution naturally at ambient conditions (almost 2 hours), again the adsorption occurs in solution up to 91.7 g S/kg sorbent of initial concentration. For comparison, the adsorption capacity of commercially used Y-Zeolite for DBT is around 6 g S/kg sorbent [46].

Further, as is indicated in Figure 20, the adsorption capacity of Cu-MOF towards 4,6-DMDBT is as high as 82.83 g S/kg sorbent at 298 K. When temperature increases by 50 K to 348 K, the adsorption capacity of Cu-MOF remains about the same at 82.83 g S/kg sorbent. After heating by an additional 40 K, the adsorption capacity still remains at 84.97 g S/kg sorbent. Finally, by cooling our solution naturally at ambient conditions (almost 2 hours), the adsorption capacity in the solution reaches 83.1 g S/kg sorbent. As

compared to the reported literature values of the adsorption capacity of aromatic sulfur compounds on Cu-MOF (HKUST-1 and C300 Basolite) in alkane solvents [46, 49, 51], one can see that we observe rather high adsorption capacities in common units of g S per kg MOF sorbent at the same temperature (typically 298 K) and at comparable initial concentrations in solution. For example, the adsorption capacity of DBT on C300 MOF as measured by us at 298 K is 78 g/kg, while the one reported by *G. Blanco et al* [46] is 45 g/kg. The published adsorption capacity of 45 g/kg was measured within the saturation range of adsorption isotherm, and thus represents the highest possible capacity. The higher adsorption capacity of 78 g/kg we observed could be because of our choice of linear alkane n-tetradecane as a solvent, instead of the reported isooctane.

3.5 Stoichiometry of Adsorption Complexes

In our experiments, we assume the existence of adsorption complexes formed by each aromatic sulfur compound with Cu-MOF. The empirical Hill formula of Cu-MOF is $C_{18}H_6Cu_3O_{12}$, and molecular weight is 604.87 g/mol. First, we calculated the stoichiometry of those adsorption complexes, namely the ratios (moles of adsorbed aromatic sulfur compound) / (moles of Cu^{2+} present in MOF). Then, we considered that each mole of Cu-MOF contains Cu^{2+} as dimeric Cu_2O_8 "paddlewheel" units, so we calculated the molar ratio (moles of adsorbed aromatic sulfur compound) / (moles of Cu_2O_8 units present in MOF). Data is shown in Table 4.

Table 4 shows those calculated ratios. One can see that all aromatic sulfur compounds studied, except thiophene, form stoichiometric adsorption complexes. Namely, one mole of respective aromatic sulfur compound is adsorbed at, on average, about 1 mole of Cu_2O_8 unit of Cu-MOF at 298 K. This means that, on average, in each

"paddlewheel unit" Cu_2O_8, only one Cu^{2+} ion may interact with one molecule of aromatic sulfur compound in the adsorption complex. For thiophene, adsorption complex is not stoichiometric at 298 K. At the higher temperatures, the stoichiometry of adsorption complex of thiophene could be affected by partial evaporation of thiophene and the resultant change of mass balance in adsorption system; thus, we do not comment further on this. On the other hand, it is interesting to know that for 4,6-DMDBT, the stoichiometric 1:1 ratio in its adsorption complex is maintained at every temperature studied.

Table 4. Stoichiometric ratios (moles of adsorbed aromatic sulfur compound) / (moles of Cu_2O_8 units present in Cu-MOF).

Adsorption temperature, K	298	348	388	298 (after cooling)
Thiophene	1.39	0.64	-	-
BT	0.97	0.99	0.11	1.14
DBT	0.92	0.77	0.44	1.14
4,6-DMDBT	1	1	1	1.1

3.6 Fluorescence Spectra of Adsorption Complexes

All fluorescence measurements were conducted at the same excitation wavelength 300 nm (Figure 21). Excitation at 300 nm corresponds to the absorption maximum of BT in solution (Figure 6). For solid BT, there is a very small fluorescence signal at 315 nm. This fluorescence excited at 300 nm originates from the transition from excited S_1 state to ground singlet state S_0 of the BT molecule [54]. The small height of this signal is consistent with the reported small cross-section of fluorescence for sulfur-containing aromatic heterocyclic compounds [55]. In order to measure fluorescence from Cu-MOF, we had to disperse it in $C_{19}H_{40}$, otherwise fluorescence spectra from the fine powder of Cu-MOF would have been non-comparable to those obtained from other samples such as BT that are dense solids. There is virtually no fluorescence from Cu-MOF dispersed in solid $C_{19}H_{40}$. Given that $C_{19}H_{40}$ cannot have fluorescence excited at 300 nm (no optical absorption at this wavelength), we note that there is no fluorescence from Cu-MOF.

On the other hand, mixture of BT and Cu-MOF shows a clear fluorescence peak at 315 nm, Figure 21. That signal is much stronger than the one obtained from pure solid BT (Figure 21), and it is observed at the same wavelength. Therefore, this peak has, in general, the same origin as the one observed from pure BT as the shapes of those two peaks are similar. Although formation of "surface sulfone" of DBT on surface of Cu-MOF after adsorption was reported in the XPS experiment [46], we argue that such "surface sulfone" is, most likely, an XPS artifact. In our experiments, the adsorption capacity of Cu-MOF does not decrease after adsorption/desorption of BT (Figure 17), therefore we do not expect any "deactivation" of Cu-MOF sorbent and formation of any products of surface chemical reaction that might cause fluorescence.

We explain the much higher amplitude of the peak as a result of the enhancement of weak fluorescence from BT in presence of Cu-MOF. Further, we speculate that this enhancement of fluorescence is due to formation of a molecular complex between Cu-MOF and BT. Our spectroscopic data are consistent with our observations of formation of stoichiometric adsorption complex of BT with Cu-MOF at 298 K as shown independently, Table 4.
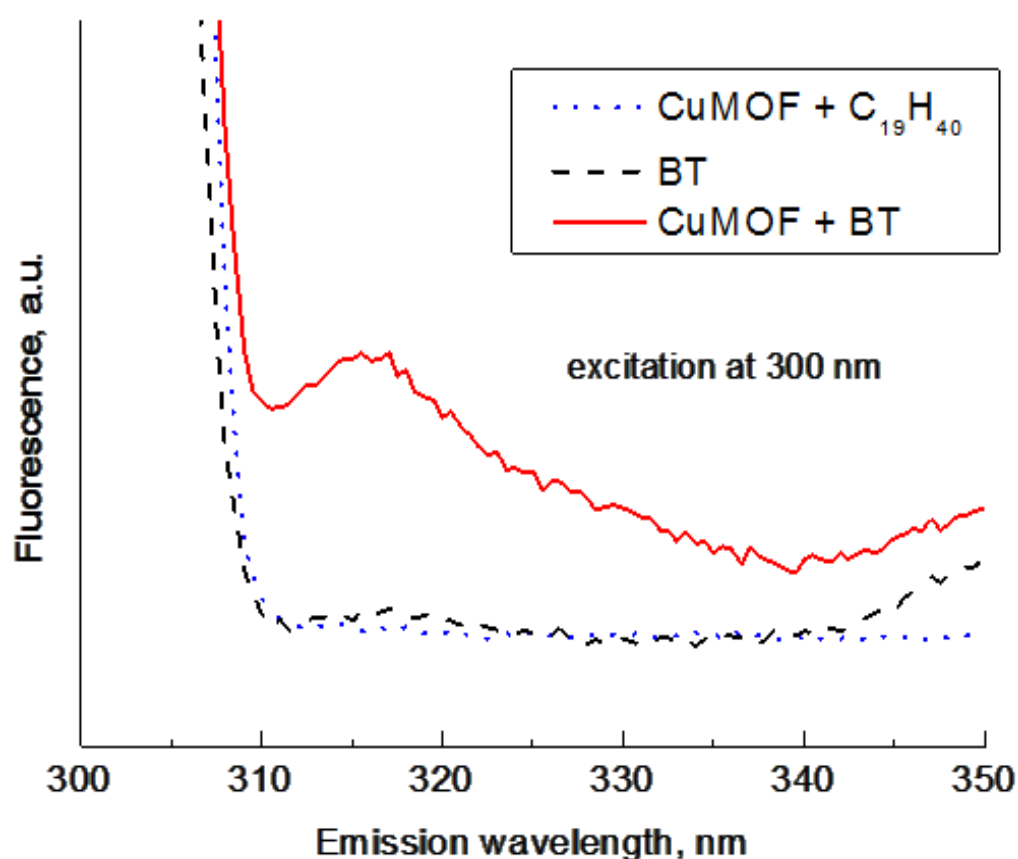

Figure 21: Fluorescence spectra of solid suspension of Cu-MOF in BT

3.7 Computational Results

Results presented in this Chapter have been obtained within the graduate course "Molecular Modeling" taught by Prof. L. Burke at Chemistry Department of Rutgers University – Camden, and taken by Muslum Demir during his graduate studies.
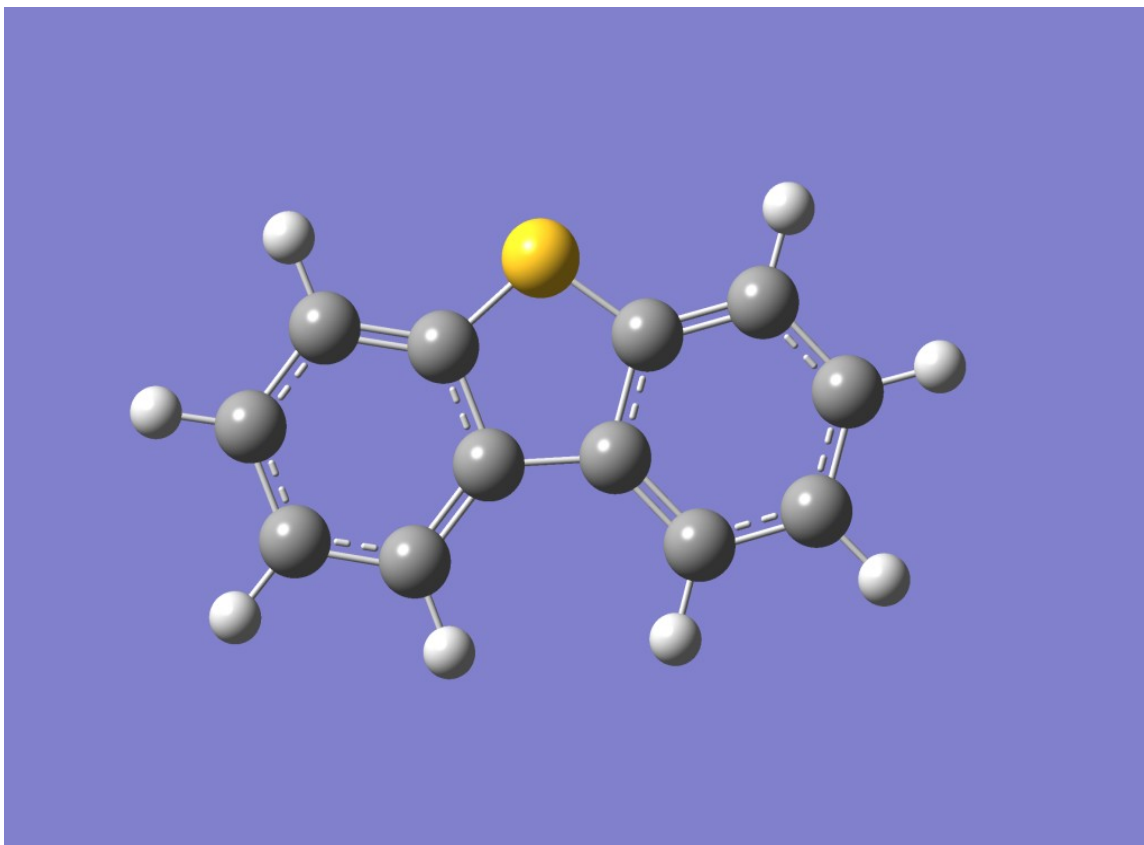
Figure 22: Gaussian view of DBT

Table 5: Bond lengths and Angles: Hartree-Fock level of the theory using the standard 6-311** basis set for optimization

Tag	Symbol	NA	NB	NC	Bond	Angle
1	C					
2	C	1			1.4038190	
3	C	2	1		1.3923663	120.6847569
4	C	3	2	1	1.3966213	118.5191789
5	C	4	3	2	1.4129027	121.6197069
6	C	1	2	3	1.3901993	120.5616043
7	H	1	6	5	1.0863357	119.7672654
8	H	2	1	6	1.0864827	119.7791585
9	H	3	2	1	1.0861359	120.7102128
10	H	6	1	2	1.0867727	120.1774398
11	C	5	4	3	2.3798949	78.8026643
12	C	11	5	4	1.3966215	156.1055514
13	C	12	11	5	1.3923663	118.5191384
14	C	13	12	11	1.4038186	120.6847949
15	C	14	13	12	1.3901995	120.5616070
16	C	15	14	13	1.4035944	119.8321774
17	H	12	11	5	1.0861359	120.7706488
18	H	13	12	11	1.0864825	119.5361367
19	H	14	13	12	1.0863363	119.6711274
20	H	15	14	13	1.0867724	120.1774313
21	S	11	5	4	1.7677606	77.8776826
-	?	16	15	14	0.9285931	167.4841917

Table 6: Bond lengths and Angles: the DFT (B3LYP) level of theory using the standard 3-21G**

basis set

Tag	Symbol	NA	NB	NC	Bond	Angle
1	C					
2	C	1			1.3988522	
3	C	2	1		1.3864475	120.6719098
4	C	3	2	1	1.3914496	118.5584805
5	C	4	3	2	1.4082162	121.6259171
6	C	1	2	3	1.3847838	120.5553984
7	H	1	6	5	1.0832241	119.7889619
8	H	2	1	6	1.0833721	119.8043701
9	H	3	2	1	1.0830837	120.6139846
10	H	6	1	2	1.0837267	120.0654917
11	C	5	4	3	2.3733223	78.8714412
12	C	11	5	4	1.3914496	156.1051357
13	C	12	11	5	1.3864475	118.5584805
14	C	13	12	11	1.3988522	120.6719098
15	C	14	13	12	1.3847838	120.5553984
16	C	15	14	13	1.3987567	119.8784361
17	H	12	11	5	1.0830837	120.8275320
18	H	13	12	11	1.0833721	119.5237175
19	H	14	13	12	1.0832241	119.6556395
20	H	15	14	13	1.0837267	120.0654917
21	S	4	3	2	1.7629928	126.0739261
-	?	5	4	3	0.9258049	73.7956880

In Tables 5 and 6, the atoms in the molecule of DBT are listed by number and element under the symbol column. The matrix entry for each atom contains the connectivity matrix indicating which atom forms chemical bonds with previously defined atoms under the Na/Length, Nb/Angle, and Nc/Dihedral columns, length of bond (Angstrom) of that atom, and angle (degrees).
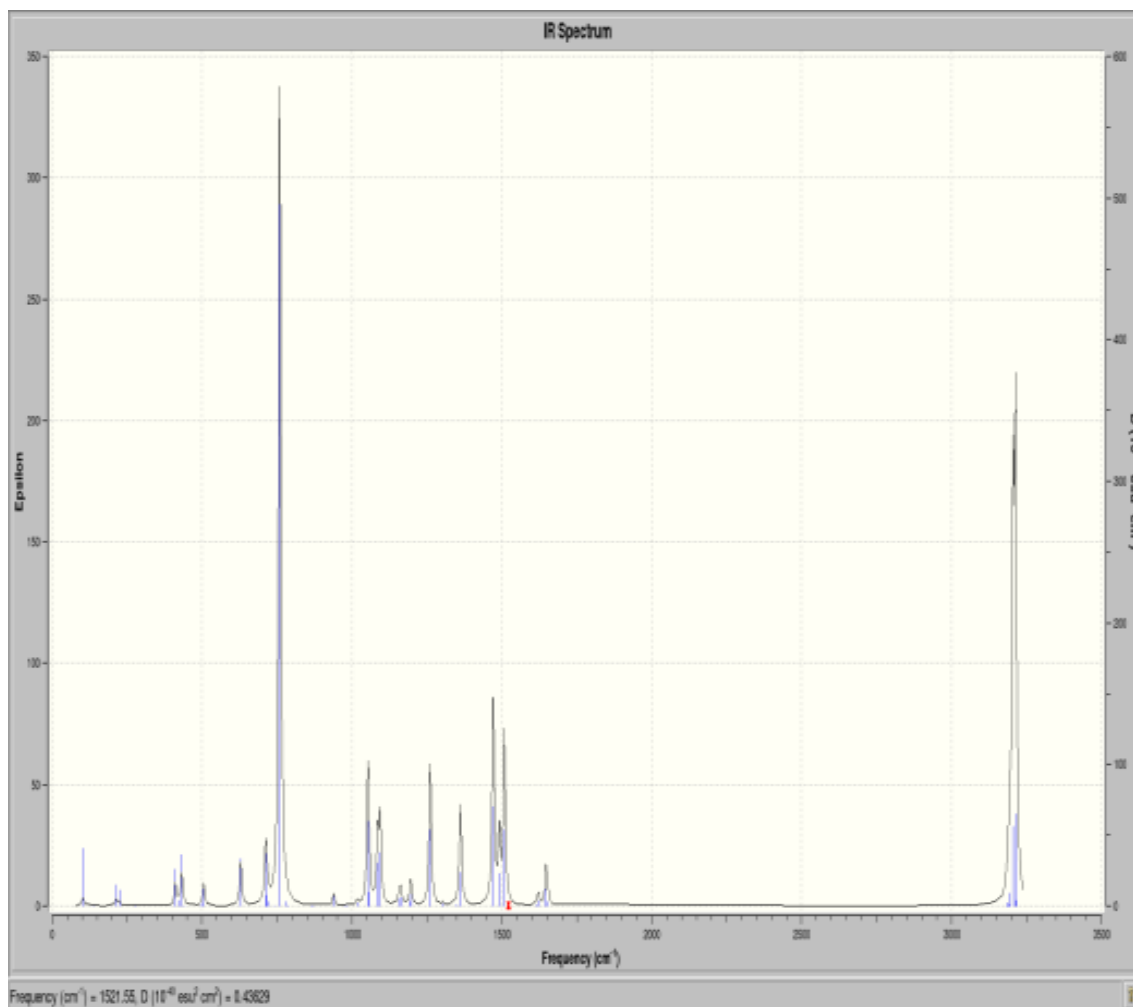
3.7.1 Calculated FTIR Spectrum

Figure 23: IR spectrum of DBT with Gaussian programming

Based on DFT (B3LYP) level of theory using the standard 6-311G** basis set for an IR spectrum, we arrive at vibrational values of 3214.35 cm^{-1} (due to C-H stretching) and 781.797 cm^{-1} (due to C-S stretching) shown on the IR spectrum of DBT in Figure 23.

3.7.2 UV/VIS Spectrum (with Gaussian program calculation)
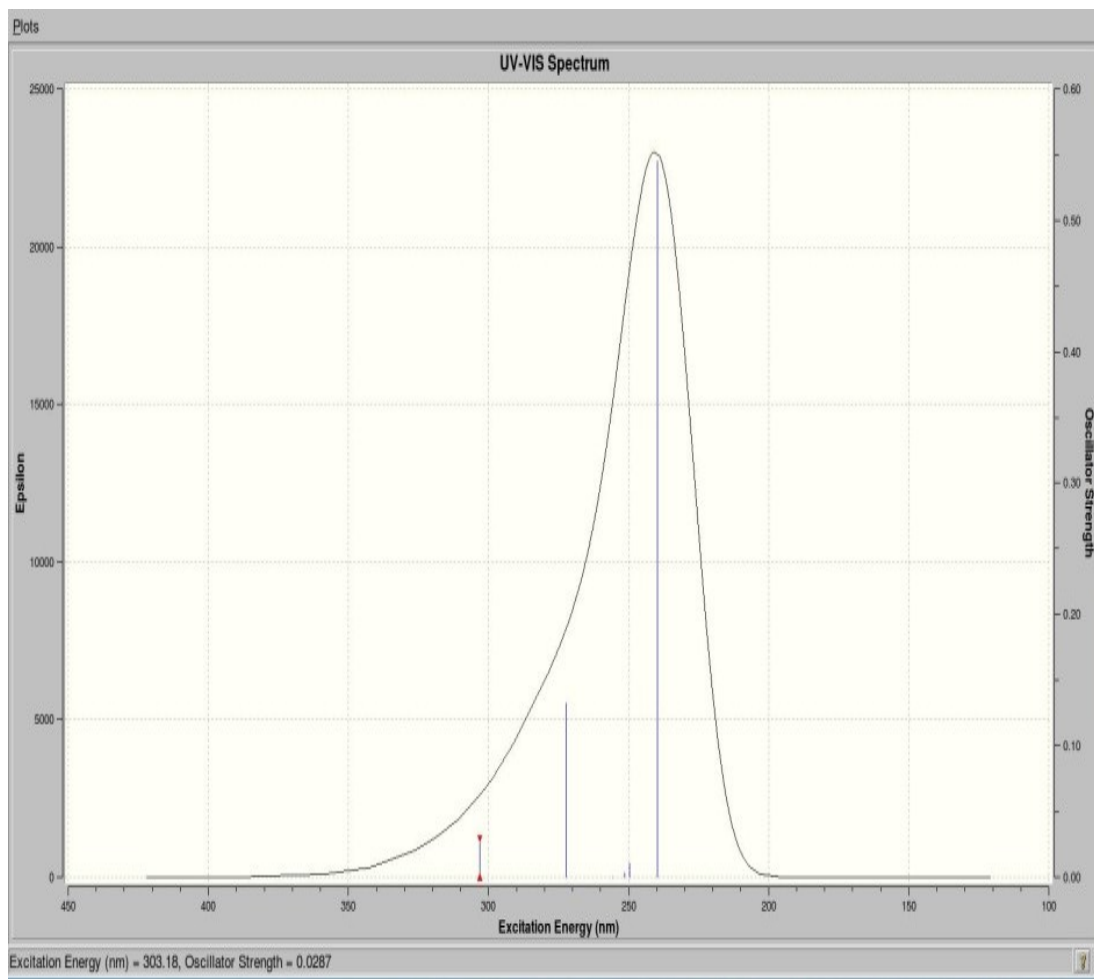

Figure 24: UV-VIS spectrum of DBT with Gaussian programming

Based on TD-DFT (B3LYP) level of theory using the standard 6-311G** basis set for UV/VIS spectrum, we arrive at electronic transition values of 239 nm, 272 nm and 303 nm in the UV-VIS spectrum of DBT in Figure 24.

3.8 Summary

MOFs are promising adsorbates for removing aromatic sulfur compounds from liquid fuels. We have investigated adsorption and desorption of typical aromatic sulfur compounds present in petroleum and liquid fuels, namely thiophene, benzothiophene (BT), dibenzothiophene (DBT), 4,6-dimethyldibenzothiophene (4,6-DMDBT) on metal-organic frameworks (MOFs). The kinetics of adsorption of the aromatic sulfur compounds studied on Cu-MOF is more complex than the first order rate law. After adsorption and desorption of these aromatic sulfur compounds on Cu-MOF, there are no products of chemical reactions with the MOF detected by UV/VIS spectroscopy and HPLC-UV. The adsorption capacity of Cu-MOF for these aromatic sulfur compounds was examined under thermodynamic equilibrium at different temperatures. Binding between Cu-MOFs and the aromatic compounds occurs via chemisorption or physisorption, depending upon the molecular structure of the compound. Formation of stoichiometric adsorption complexes between aromatic sulfur compounds and Cu-MOF was demonstrated at 298 K. Evidence of molecular interaction between Cu-MOFs and aromatic sulfur compound BT was shown by fluorescence spectroscopy. Quantum chemical simulations of the structure of aromatic sulfur compound DBT and its molecular spectra were conducted and interpreted.

Chapter 4: Future Work

Below are some areas related to our research that require more investigation.

1. The different temperature-dependent adsorption capacity of small-molecule aromatic sulfur compounds (such as BT) versus large-ring substituted compounds (such as 4,6-DMDBT) at 25-115 °C suggests that temperature changes can be used to separate those compounds when present simultaneously in solution via selective adsorption/desorption from Cu-MOF.

2. Adsorption at higher temperatures, e.g. 115-215 °C is expected to be even more selective in the separation of aromatic sulfur compounds of different molecular structure.

3. Stoichiometric adsorption complexes of aromatic sulfur compounds with Cu-MOF have been shown to be formed at high concentrations of aromatic sulfur compounds (e.g. 0.02 M) in solution. A next step is to determine if the adsorption complexes would remain stoichiometric even when formed from diluted solutions (e.g. 0.002 M).

4. The structure of adsorption complexes needs to be further proven by molecular spectroscopy such as Raman and fluorescence spectroscopy.

Chapter 5: List of Presentations and Publications Resulting from Research Work or Described in This Thesis

1) 'Adsorption and desorption of thiophenes from model liquid fuel on Cu-containing MOF', M. Demir and A. Samokhvalov, submitted to *Fuel Journal.*

2) 'Mechanisms of Adsorptive Desulfurization of Liquid Fuels with Cu- MOF by Experiment and Simulation' M. Demir, M.L. McKee and A. Samokhvalov, recently accepted for presentation at the *23rd North American Catalysis Society Meeting*, June 2013.

3) 'Adsorption of aromatic sulfur compounds by metal-organic frameworks', M. Demir A. Samokhvalov, presented and published at *Philadelphia Section of the American Chemical society, The 13th Student Poster sessions, retrieved from http://philadelphia.sites.acs.org/events_info/2013_events/StudentPosterSession.pdf*

4) 'Kinetics and Mechanism of Adsorption of Aromatic Sulfur Compounds on MOFs from Liquid Fuels', A. Samokhvalov, and M. Demir presented at *AIChE Annual Meeting, Pittsburg, October 2012.*

5) 'Adsorption of aromatic sulfur compounds on metal-organic frameworks' M. Demir A. Samokhvalov, presented at *Poster Session ACS Annual Meeting, Philadelphia, August* 2012.

6) 'Adsorption of unwanted highly aromatic sulfur compounds by metal-organic frameworks', M. Demir A. Samokhvalov, presented as a poster session and published as an abstract review at *Philadelphia Section of the American Chemical society, The 12th Student Poster sessions, page 18, 2012.*

Chapter 6: References

1 A.L. Boehman, J. Song, *Energy and Fuels*, 2005, 19, 5, 1857–1864.

2 C. Song, *Catalysis Today*, 2003, 86, 211–263.

3 K. Knudsen, B.H. Cooper, H. Topsoe, *Applied Catalysis A-General*, 1999, 189, 2, 205-215.

4 E. Ito, J.A. Rob van Veen, *Catalysis Today*, 2006, 116, 4, 446-460.

5 A. Samokhvalov, B.J. Tatarchuk, *Catalysis Reviews-Science and Engineering,* 2010*, 52, 381-410.*

6 F.P. Richter, A.L. Williams, S.L. Meisel, *J. American Chemical Society*, 1956, 78, 2166–2167.

7 R.E. Connick, R.E. Poulsen, *J. Physical Chemistry*, 1959, 63, 568.

8 Fact Sheet, U.S. Tar Sands Potential, 2006, retrieved from http://www.circleofblue.org/waternews/wpcontent/uploads/2010/08/Tar_Sands_Fact_Sheet.pdf

9 S. Yui, *J. The Japan Petroleum Institute,* 2008, 51, 1-13.

10 K.O. Blumberg, M.P. Walsh, C. Pera, The International Council on Clean Transportation (I.C.C.T.), Boston, 2003, 1-66, retrieved from http://www.theicct.org/sites/default/files/publications/Low-Sulfur_ICCT_2003.pdf.

11 J.G. Speight, "*Chemistry and Technology of Petroleum*", CRC Press, Boca Raton, 1999.

12 D.S. Stratiev, I.T. Shishkova, P.Z. Tzingov, *Industrial and Engineering Chemistry Research,* 2009, 48, 10253-10261.

13 T.V. Choudhary, *Industrial and Engineering Chemistry Research*, 2007, 46, 8363-8370.

14 C. Yin, D. Xia, *Fuel*, 2004, 83, 433-441.

15 X. Zeng, J. Lin, J. Liu, Y. Yang, Chin. *J. Analytical Chemistry*, 2006, 34, 1546-1551.

16 T. Schade, J. T. Andersson, *Energy and Fuels*, 2006, 20, 1614-1620.

17 A. Stanislaus, A. Marafi, M.S. Rana, *Catalysis Today*, 2010, 153, 1-68.

18 D. I. Stern, *Chemosphere*, 2005, 58, 163-175.

19 A. Ololade, *Bulletin of Environmental Contamination and Toxicology*, 2010, 85, 238-242.

20 J. Payne, C. Phillips, *Environmental Science and Technology*, 1985, 19, 569-579.

21 T. J. Crone, M. Tolstoy, *Science*, 2010, 330, 634-634.

22 F. Berthou, V. Vignier, *International J. Environmental Analytical Chemistry*, 1986, 27, 81-96.

23 V. Coropceanu, O. Kwon, B. Wex, B. R. Kaafarani, N. E. Gruhn, J. C. Durivage, D. C. Neckers, *Chemistry A European J.*, 2006, 12, 2073-2080.

24 E. Block, *ACS Symposium Series*, 1981, 158, 3-16, DOI: http://pubs.acs.org/doi/pdf/10.1021/bk-1981-0158.ch001.

25 D. Lednicer, "*Strategies for Organic Drug Synthesis and Design*", Wiley, Interscience, New York, 1998.

26 A. Samokhvalov, L. Hong, Y. Liu, J. Garguilo, R. J. Nemanich, G. S. Edwards, J. D. Simon, *Photochemistry and Photobiology*, 2005, 81, 145–148.

27 M. Ribeiro da Silva, A. Santos, *J. Thermal Analysis and Calorimetry*, 2009, 95, 333-344.

28 N.K. Nag, D. Fraenkel, J. A. Moulijn, B. C. Gates, *J. Catalysis*, 1980, 66, 162.

29 M. Houalla, D. H. Broderick, A. V. Sapre, N. K. Nag, V.H.J. de Beer, B. C. Gates, H. Kwart, *J. Catalysis*, 1980, 61, 523.

30 C. Kwak, J.J. Lee, J.S. Bae, K. Choi, S. H. Moon, *Applied Catalysis General*, 2000, 200, 233-242.

31 M.R. Hoffmann, S.T. Martin, W. Choi, D.W. Bahnemannt, *Chemical Reviews.*, 1995, 95, 69-96.

32 S.C. Roy, O.K. Varghese, M. Paulose, C.A. Grimes, *ACS Nano*, 2010, 4, 1259-1278.

33 A.J. Bard, *Science*, 1980, 207, 139-144.

34 D. Xu, D. Zhao, D. Chen, Y.E. Song, *Chemistry European J.*, 2012, 18, 4775-4781.

35 P. Ruiz, B. Delmon, "*Studies in Surface Science and Catalysis*", Elsevier, 1992.

36 R. Vidyalakshmi, R. Paranthaman, R. Bhakyaraj, *J. Agricultural Sciences*, 2009, 5, 3, 270-278.

37 M. Soleimani, A. Bassi, A. Margaritis, *Biotechnology Advances*, 2007, 25, 6, 570-596.

38 A.J. Hernández-Maldonado, *Catalysis Reviews-Science and Engineering,* 2004, 46, 111-150.

39 R.T. Yang, A.J. Hernández-Maldonado, F.H. Yang, *Science*, 2003, 301, 79-81.

40 L. Ma, R.T. Yang, *Industrial and Engineering Chemistry Research*, 2007, 46, 8938-8945.

41 J.H. Kim, X. Ma, A. Zhou, C. S., Song, *Catalysis Today*, 2006, 111, 74-83.

42 C. Prestipino, L. Regli, J.G. Vitillo, F. Bonino, A. Damin, C. Lamberti, A. Zecchina, P.L. Solari, K.O. Kongshaug, S. Bordiga, *Chemistry of Materials*, 2006, 18, 5, 1337-1346.

43 O.Yaghi, C.E. Davis, H. Li, *J. American Chemical Society,* 1997, 119, 2861-2868.

44 A. Stein, *Advanced Materials*, 2003, 15, 763-775.

45 G. Ferey, *Chemistry of Materials,* 2001, 13, 3084-3098.

46 G. Blanco-Brieva, J.M. Campos-Martin, S.M. Al-Zahrani, J.L.G. Fierra, *Fuel*, 2011, 90, 190-197.

47 S. Klaus, K. Tobias, K. Stefan, *Microporous and Mesoporous Materials*, 2004, 73, 81-88.

48 J.A. Moulijn, A.E. van Diepen, and F. Kapteijn, *Applied Catalysis. A: General*, 2001, 212, 1-2, 3-16.

49 K. A. Cychosz, A. G. Wong-Foy, and A. J. Matzger, *J. American Chemical Society*, 2008, 130, 6938-6939.

50 S. Suezer, *Applied Spectroscopy, 2000, 54, 1716-1718.*

51 B. Liu, Y. Zhu, S. Liu, and J. Mao, *J. Chemical Engineering Data*, 2012, 57, 4, 1326-1330.

52 X. Ma, L. Sun, and C. Song, *Catalysis Today,* 2002, 77, 1-2, 107-116.

53 E.G. Werner, *Recueil des Travaux Chimiques Pays-Bas*, 1949, 68, 509-519.

54 S.G. McKinley, R.J. Angelici, *Chem. Commun.,* 2003, 2620-2621.

55 L. Alvarez-Valtierra, T. Yi, W. David, *J. Physical Chemistry A*, 2009, 113, 11, 2261-2267.